

RECEIVED: July 28, 2023

ACCEPTED: September 27, 2023

PUBLISHED: October 6, 2023

Search for new physics in multijet events with at least one photon and large missing transverse momentum in proton-proton collisions at 13 TeV



The CMS collaboration

E-mail: cms-publication-committee-chair@cern.ch

ABSTRACT: A search for new physics in final states consisting of at least one photon, multiple jets, and large missing transverse momentum is presented, using proton-proton collision events at a center-of-mass energy of 13 TeV. The data correspond to an integrated luminosity of 137 fb^{-1} , recorded by the CMS experiment at the CERN LHC from 2016 to 2018. The events are divided into mutually exclusive bins characterized by the missing transverse momentum, the number of jets, the number of b-tagged jets, and jets consistent with the presence of hadronically decaying W, Z, or Higgs bosons. The observed data are found to be consistent with the prediction from standard model processes. The results are interpreted in the context of simplified models of pair production of supersymmetric particles via strong and electroweak interactions. Depending on the details of the signal models, gluinos and squarks of masses up to 2.35 and 1.43 TeV, respectively, and electroweakinos of masses up to 1.23 TeV are excluded at 95% confidence level.

KEYWORDS: Beyond Standard Model, Hadron-Hadron Scattering , Supersymmetry

ARXIV EPRINT: [2307.16216](https://arxiv.org/abs/2307.16216)

Contents

| | | |
|------------------------------|--|-----------|
| 1 | Introduction | 1 |
| 2 | The CMS detector and event reconstruction | 4 |
| 3 | Collision and simulated data sets | 6 |
| 4 | Event selection | 7 |
| 5 | Background estimation | 9 |
| 5.1 | Lost-lepton background | 9 |
| 5.2 | Misidentification of electrons as photons | 11 |
| 5.3 | $Z(vv)\gamma + \text{jets}$ background | 13 |
| 5.4 | $\gamma + \text{jets}$ and QCD multijet background | 14 |
| 6 | Systematic uncertainties | 15 |
| 7 | Results and interpretation | 16 |
| 8 | Summary | 20 |
| A | Predicted and observed events | 22 |
| The CMS collaboration | | 29 |

1 Introduction

Several extensions of the standard model (SM) of elementary particles attempt to provide an explanation for the origin of dark matter (DM) [1, 2] and to resolve the gauge hierarchy problem [3–6]. Supersymmetry (SUSY) [7–14] is a hypothesized symmetry between fermions and bosons, which, when included in extensions to the SM, predicts a new bosonic (fermionic) superpartner for each SM fermion (boson). In SUSY models with R -parity conservation [15], the lightest supersymmetric particle (LSP) is stable and often neutral and weakly interacting, making it a possible DM candidate. In addition, gauge coupling unification is a natural possibility in supersymmetric theories [16].

Superpartners would contribute to quantum corrections to the Higgs boson (H) mass such that the H mass parameter would have only a logarithmic dependence on the scale of new physics. This effect could reduce the need for fine-tuning of the H mass [6], thereby preserving naturalness, if the superpartners with the largest contributions to the corrections are sufficiently light. These particles include the gluino, top squark, and bottom squark, which are the superpartners of the SM gluon, top quark, and bottom quark, respectively.

If those color-charged superpartners are not accessible at the LHC, SUSY may still satisfy naturalness conditions if the higgsino, the superpartner of the Higgs boson, is near the electroweak scale [17].

This paper explores the signatures of SUSY particles produced via strong and electroweak interactions in proton-proton (pp) collisions, with a particular focus on final states containing at least one photon, multiple jets, and large missing transverse momentum. In gauge-mediated SUSY-breaking scenarios, the LSP is a gravitino (\tilde{G}), the superpartner of the graviton, and it is expected to be roughly a few GeV in mass [18, 19]. If the next-to-LSP (NLSP) is a chargino (neutralino), its decay will result in a W boson (photon, Z boson, or Higgs boson) and a \tilde{G} . The neutralino is an admixture of neutral wino, bino, and/or higgsino components that can couple to photons. Such decays are especially prominent if sleptons, the superpartners of SM leptons, are sufficiently massive that decays to sleptons are suppressed.

We interpret the results of this search using simplified models [20–24] of SUSY particle production via strong and electroweak interactions. Specifically, we consider several models of squark- and gluino-mediated production of charginos and neutralinos, in which each of the latter particles subsequently decays to the LSP and an SM boson. We also consider the production of neutralinos and charginos, collectively referred to as electroweakinos, via electroweak interactions. In all simplified models considered in this paper, the decays of SUSY particles are assumed to be prompt, and the mass of the gravitino, $m_{\tilde{G}}$, is fixed to be 1 GeV. The event kinematic properties do not depend strongly on the exact choice of $m_{\tilde{G}}$ in the phase space explored in this analysis. This search therefore targets final states with at least one photon produced from the decay of a neutralino and missing transverse momentum from the LSP, which escapes the collision region without detection.

Representative diagrams depicting simplified models [24] of gluino (\tilde{g}) pair production and top squark (\tilde{t}) pair production are shown in figure 1. In the gluino pair production models, the gluino decays to a neutralino ($\tilde{\chi}_1^0$) and a pair of quarks; any possible $\tilde{\chi}_1^0$ decays occur with equal probability. The T5qqqHG model is defined by the decay of gluinos to a pair of light-flavored quarks ($q\bar{q}$) and $\tilde{\chi}_1^0$, followed by $\tilde{\chi}_1^0 \rightarrow H\tilde{G}$ or $\tilde{\chi}_1^0 \rightarrow \gamma\tilde{G}$ with 50% branching fraction each. The mass of the $\tilde{\chi}_1^0$ is taken to be 127 GeV or above. In the T5bbbbZG and T5tttZG models, $\tilde{g} \rightarrow b\bar{b}\tilde{\chi}_1^0$ and $\tilde{g} \rightarrow t\bar{t}\tilde{\chi}_1^0$, respectively, and the $\tilde{\chi}_1^0$ decays to $Z\tilde{G}$ or $\gamma\tilde{G}$ with 50% branching fraction each. In the top squark pair production model T6ttZG, each top squark decays to a top quark and a $\tilde{\chi}_1^0$, followed by a decay $\tilde{\chi}_1^0 \rightarrow Z\tilde{G}$ or $\tilde{\chi}_1^0 \rightarrow \gamma\tilde{G}$ with 50% branching fraction each. In the models involving $\tilde{\chi}_1^0 \rightarrow Z\tilde{G}$, $\tilde{\chi}_1^0$ masses as low as 10 GeV are considered.

Example diagrams for chargino-neutralino ($\tilde{\chi}_1^\pm\tilde{\chi}_1^0$) and chargino-chargino ($\tilde{\chi}_1^\pm\tilde{\chi}_1^\mp$) production are presented in figure 2, and the models are denoted TChiWG and TChiNG, respectively. In both models, the charginos and neutralinos are degenerate in mass. In the TChiWG model, the branching fractions for $\tilde{\chi}_1^0 \rightarrow \gamma\tilde{G}$ and $\tilde{\chi}_1^\pm \rightarrow W\tilde{G}$ are taken to be 100%. The TChiNG model includes all electroweak production modes of nearly degenerate triplet of chargino and neutralino states: $\tilde{\chi}_1^\pm\tilde{\chi}_1^\mp$, $\tilde{\chi}_1^\pm\tilde{\chi}_1^0/\tilde{\chi}_1^\pm\tilde{\chi}_2^0$, and $\tilde{\chi}_1^0\tilde{\chi}_2^0$. The $\tilde{\chi}_1^\pm$ and $\tilde{\chi}_2^0$ decay to $\tilde{\chi}_1^0$ and low-momentum particles that are outside the kinematic acceptance of this analysis. The $\tilde{\chi}_1^0$ decays to $\gamma\tilde{G}$, $Z\tilde{G}$, and $H\tilde{G}$ with branching fractions of 50, 25, and 25%,

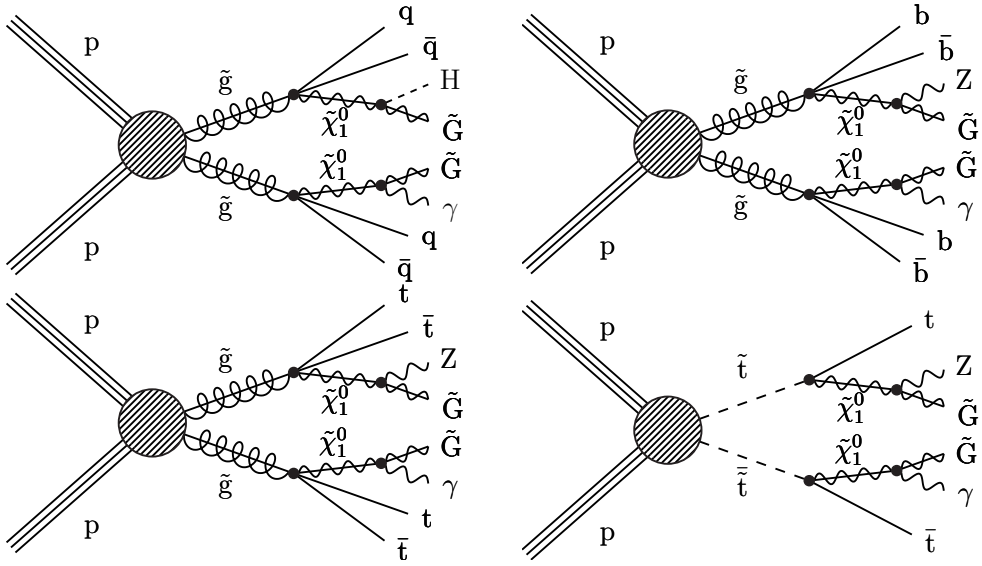


Figure 1. Diagrams of simplified models of gluino pair production: T5qqqqHG (upper left), T5bbbbZG (upper right), T5ttttZG (lower left), and top squark pair production: T6tttZG (lower right). The models are defined in the text.

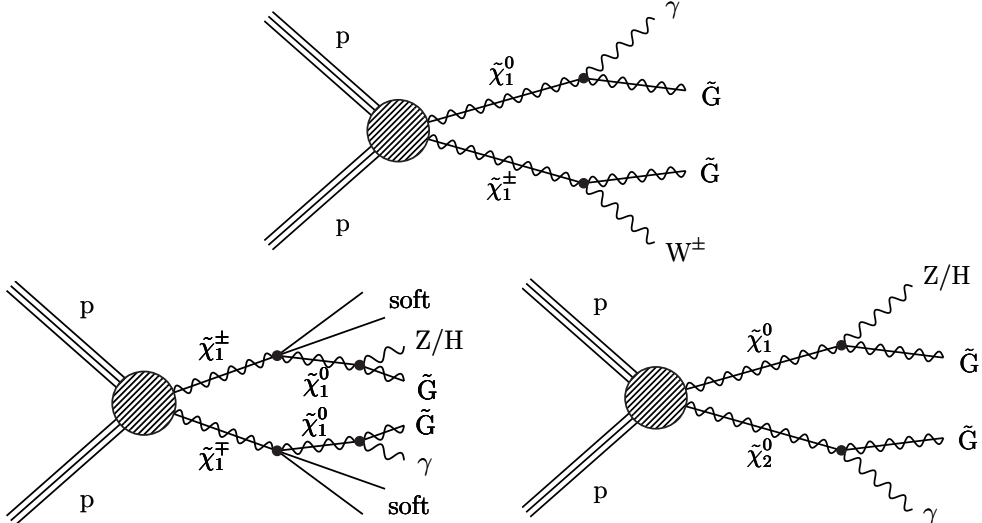


Figure 2. Diagrams of simplified models of electroweakino pair production: TChiWG (upper), TChiNG (lower left), and TChiNGnn (lower right). Only the $\tilde{\chi}_1^\pm \tilde{\chi}_1^0$ and $\tilde{\chi}_1^\pm \tilde{\chi}_1^\mp$ cases are shown for the TChiWG and TChiNG models, respectively. The models are defined in the text. “Soft” indicates particles with momentum too low to be detectable.

respectively. Additionally, there is a scenario denoted TChiNGnn, where $\tilde{\chi}_1^0$ decays to $Z\tilde{G}$ and $H\tilde{G}$ with 50% branching fraction each, and $\tilde{\chi}_2^0$ decays to $\gamma\tilde{G}$ with 100% branching fraction. Only the $\tilde{\chi}_1^0\tilde{\chi}_2^0$ process contributes to this scenario.

Previous searches by the CMS Collaboration for signatures of squark, gluino, and electroweakino production involving photons with data corresponding to an integrated

luminosity of 36 fb^{-1} at $\sqrt{s} = 13\text{ TeV}$ are documented in refs. [25–27]. Similar searches have also been reported by the ATLAS Collaboration based on data corresponding to integrated luminosities of 36 [28, 29] and 139 fb^{-1} [30]. The present search follows the analysis strategy used in ref. [27]. The search regions are reoptimized based on the availability of four times more data and are extended to include jets consistent with hadronic decays of W , Z , or Higgs bosons for electroweakino searches.

This paper is structured as follows. A brief description of the CMS detector and event reconstruction is given in section 2. The data sets are described in section 3 and the event selection in section 4. The methods used to estimate SM backgrounds are presented in section 5 and the systematic uncertainties in the predictions are provided in section 6. The results and summary are presented in sections 7 and 8, respectively. Tabulated results are provided in the HEPData record for this search [31].

2 The CMS detector and event reconstruction

The central feature of the CMS apparatus is a superconducting solenoid of 6 m internal diameter, providing a magnetic field of 3.8 T . Within the solenoid volume are a silicon pixel and strip tracker, a lead tungstate crystal electromagnetic calorimeter (ECAL), and a brass and scintillator hadron calorimeter, each composed of a barrel and two endcap sections. The tracker systems cover a pseudorapidity range of $|\eta| < 2.5$, and the calorimeter systems cover $|\eta| < 3.0$. Forward calorimeters extend the coverage provided by the barrel and endcap detectors up to $|\eta| < 5.2$. Muons are measured in gas-ionization detectors embedded in the steel flux-return yoke outside the solenoid. A more detailed description of the CMS detector, together with a definition of the coordinate system used and the relevant kinematic variables, can be found in ref. [32]. Events of interest are selected using a two-stage trigger system, described in ref. [33].

Collision events are reconstructed using the particle-flow (PF) algorithm [34] which combines information from various subdetectors in an optimized way to give a list of PF candidates, namely photons, electrons, muons, charged hadrons, and neutral hadrons. Charged-particle tracks are used to reconstruct pp interaction vertices in the event. The primary vertex is taken to be the vertex corresponding to the hardest scattering in the event, evaluated using tracking information alone, as described in section 9.4.1 of ref. [35]. This vertex is required to be within 24 cm of the center of the detector in the z direction, and within 2 cm in the transverse direction. The remaining reconstructed vertices are referred to as pileup vertices and correspond to additional pp interactions in the same bunch crossing.

Reconstructed PF candidates are clustered into jets using the infrared and collinear safe anti- k_T algorithm [36, 37] with a distance parameter of 0.4 (0.8), referred to as AK4 (AK8) jets. The pileup contribution to the AK4 jet momentum is mitigated by discarding all the charged-particle tracks associated with pileup vertices and applying an offset correction to mitigate the average contribution of neutral particles [38, 39]. To mitigate the effect of pileup interactions on the AK8 jet momentum, a pileup per particle identification algorithm [39] is used, which makes use of local shape information to distinguish particles originating from hard scatter and pileup interactions. To account for the nonuniformity

of the detector response across the jet p_T and η ranges, jet energy corrections (JECs) are derived from the simulation in order to make the response of reconstructed jets equal to the particle-level jets on average. Residual differences in response between data and simulation are corrected based on dedicated measurements of the momentum balance in dijet, γ +jet, Z+jet, and multijet events [40]. The jet energy resolution (JER) in the simulation is also modified by smearing the jet p_T , using scale factors derived from data ranging from 1.1–1.2. Jets potentially dominated by contributions from anomalous detector signals or reconstruction failures are discarded using dedicated jet identification (ID) criteria [41]. The AK4 jets used in this search are required to have $p_T > 30 \text{ GeV}$ and $|\eta| < 2.4$.

The hadronization products from a hadronic decay of an energetic W, Z, or Higgs boson can be clustered into a single wide jet, which is reconstructed as an AK8 jet. The AK8 jets considered in this search are required to have $p_T > 200 \text{ GeV}$ and $|\eta| < 2.4$. The AK8 jet mass, m_J , is reconstructed using the soft-drop algorithm [42], which improves jet mass resolution by removing soft and wide-angle contributions. Requirements are applied to m_J to identify W, Z, or Higgs boson candidates. The same requirement $65 < m_J < 105 \text{ GeV}$ is used for both W and Z bosons, as the difference in the particle masses is smaller than the m_J resolution; jets that pass this requirement are called V-tags, where V = W or Z. For Higgs bosons, the requirement $105 < m_J < 140 \text{ GeV}$ is applied, and passing jets are called H-tags.

Jets originating from b quarks are identified by a combined secondary vertex algorithm based on a deep neural network (DEEPCSV), applied to the reconstructed AK4 jets [43]. A medium working point is used for the DEEPCSV discriminator. This corresponds to a b jet tagging efficiency of 65% for jets with $p_T > 30 \text{ GeV}$ with corresponding misidentification probability for gluon and light-quark (charm-quark) jets of 1.6% (13%).

The negative vector \vec{p}_T sum of all PF particles is defined as the \vec{p}_T^{miss} , and its magnitude is the missing transverse momentum (p_T^{miss}) used in this analysis. The \vec{p}_T^{miss} is corrected for the changes in the \vec{p}_T of jets after applying JECs. Events in which p_T^{miss} is identified to be originating from a mismeasured jet, detector noise, nonfunctional calorimetric channels, or reconstruction failures are rejected by dedicated algorithms [44]. Events with $p_T^{\text{miss}} > 200 \text{ GeV}$ are used in this analysis.

In order to improve the quality of the PF reconstruction, additional identification criteria are applied to photon candidates [45]. To suppress the misidentification of neutral pions, which are copiously produced in jets, as photons, the reconstructed photon candidates are required to be isolated. The isolation variable is defined as the p_T sum of a given type of PF particle candidate within a cone of radius $\Delta R = 0.3$, where $\Delta R = \sqrt{(\Delta\eta)^2 + (\Delta\phi)^2}$ and ϕ is the azimuthal angle in radians, around the direction of the photon, excluding the photon itself. Separate isolation sums are computed for charged hadrons, photons, and neutral hadrons. The isolation sums are adjusted using η -dependent effective-area corrections, which account for the variation of energy density in a given event based on pileup interactions [45]. The charged-hadron isolation sum is required to be less than 1.694 (2.089) GeV for photons in the ECAL barrel (endcap); the requirements for the other isolation sums are expressed as linear or quadratic functions of the photon p_T for photon or neutral-hadron isolation, respectively. Isolated photons with $p_T > 100 \text{ GeV}$ and $|\eta| < 2.4$, excluding the ECAL barrel-endcap transition region $1.44 < |\eta| < 1.56$, are considered for

further analysis. The efficiency of the photon identification and isolation requirements is 90% and the misidentification rate is 15–25%.

As with photons, additional identification criteria are applied to electron [45] and muon [46] candidates. The electron and muon candidates are also required to have $p_T > 10\text{ GeV}$ and to be isolated, based on a variable defined as the scalar p_T sum of the charged hadron, neutral hadron, and photon PF candidates within a variable-radius cone around the lepton direction, divided by the lepton p_T . The expected contributions of neutral particles from pileup interactions are subtracted from the isolation sum [38]. The radius of the cone is 0.2 for lepton $p_T < 50\text{ GeV}$, $10\text{ GeV}/p_T$ for $50 < p_T < 200\text{ GeV}$, and 0.05 for $p_T > 200\text{ GeV}$. The decreasing radius of the cone with lepton p_T is motivated by the increased collimation of the decay products from the lepton’s parent particle with increasing Lorentz boost and helps to retain high lepton isolation efficiency in events with large number of jets or pileup interactions. The isolation variable is required to be less than 0.1 (0.2) for electrons (muons).

Charged-particle tracks, subsequently referred to as tracks, are used to reject events potentially containing hadronic decays of τ leptons; electrons or muons that could not be identified with the criteria described earlier; and low-momentum leptons from hadron decays. An isolation requirement is applied to these tracks, based on the p_T sum of other tracks within a cone of 0.3 around each track. The isolation sum divided by the track p_T is required to be less than 0.2 (0.1) for tracks identified as a PF electron or muon (PF charged hadron). The leptonic tracks are required to have $p_T > 5\text{ GeV}$ and the hadronic tracks $p_T > 10\text{ GeV}$, along with the transverse mass between the track p_T and p_T^{miss} , defined as $m_T = \sqrt{2p_T^\ell p_T^{\text{miss}}(1 - \cos \Delta\phi)}$, less than 100 GeV . Here, $\Delta\phi$ is the angular separation between the track \vec{p}_T and the \vec{p}_T^{miss} . This m_T requirement preferentially selects isolated tracks from $W \rightarrow \ell\nu$ decays.

3 Collision and simulated data sets

We select collision events that are recorded based on the p_T^{miss} reconstructed at the trigger level. The trigger-level p_T^{miss} threshold varies from $90\text{--}140\text{ GeV}$ for the data set used in this search. The efficiencies of these p_T^{miss} triggers are measured using data sets recorded with single-electron triggers, as a function of the reconstructed p_T^{miss} . Trigger efficiencies for events with reconstructed p_T^{miss} of at least 200 (300) GeV are found to be 70, 60, and 60% (95, 95, and 97%) for data collected in 2016, 2017, and 2018, respectively. In addition to the p_T^{miss} -triggered data set, single-electron and single-muon data sets are also used for the estimation of the background from electrons misidentified as photons, described in section 5.2. The estimation of backgrounds primarily relies on observed data, with Monte Carlo (MC) events used to derive correction factors and scale factors, to validate various background estimation methods, and to assess systematic uncertainties.

We use the MADGRAPH5_aMC@NLO event generator (version 2.2.2 for 2016, and 2.4.2 for 2017–2018) [47, 48] at leading order (LO) precision for simulating the production of the $t\bar{t} + \text{jets}$, $W + \text{jets}$, $Z + \text{jets}$, QCD multijet, and $W\gamma$ processes and at next-to-LO (NLO) precision for the $t\bar{t}\gamma$ process. The $t\bar{t}\gamma$ events are simulated with up to one additional parton

at the matrix element level, while the $W\gamma$ events have up to two additional partons, the $t\bar{t} + \text{jets}$ events up to three additional partons, and the other samples up to four additional partons. The single top quark process is modeled at NLO in perturbative QCD, with MADGRAPH5_aMC@NLO used for s -channel production. Signal events are generated with the MADGRAPH5_aMC@NLO generator at LO precision in a manner similar to the SM backgrounds, with up to two additional partons at the matrix element level. The decays of gluinos, top squarks, and neutralinos are modeled with PYTHIA8 [49].

The NNPDF3.0 LO (NLO) parton distribution functions (PDFs) are used for samples simulated at LO (NLO) precision that correspond to the 2016 data [50]. The NNPDF3.1 next-to-NLO (LO) PDFs are used for all 2017–2018 simulated background (signal) samples [51]. Parton showering and hadronization are performed for background samples using the PYTHIA 8.212 generator [49] with the CUETP8M1 underlying event tune [52] for 2016 and PYTHIA 8.226 (8.230) with the CP5 underlying event tune for 2017 (2018) [53]. For the signal samples, the CUETP8M1 (CP2) underlying event tune and PYTHIA version 8.226 (8.230) are used for 2016 (2017–2018). Partons generated with MADGRAPH5_aMC@NLO and PYTHIA that would otherwise be counted twice are removed using the MLM [48] and FxFx [54] matching schemes in LO and NLO samples, respectively. The cross sections used for normalizing the signal yields are computed at NLO plus next-to-leading logarithmic (NLL) precision [55–61].

The SM MC events are processed through a detailed simulation of the CMS detector based on the GEANT4 [62] software. The simulated events are then reconstructed using the same algorithms as used for the collision data. The detector simulation of signal events is performed with the CMS fast simulation package [63, 64]. The signal samples are corrected for differences with respect to the GEANT4-based simulation. Both the SM background samples and the signal samples are generated with nominal distributions of the number of pileup interactions, which are then reweighted to match the distribution measured in data.

4 Event selection

Events are selected using a set of criteria, referred to as the baseline selection, summarized in table 1. The events are required to have $p_T^{\text{miss}} > 300 \text{ GeV}$, and $N_{\text{jets}} \geq 2$, where N_{jets} is the number of AK4 jets with $p_T > 30 \text{ GeV}$ and $|\eta| < 2.4$. The events must also contain at least one photon with $p_T > 100 \text{ GeV}$ and $|\eta| < 2.4$. The photons are required to be separated from the jets by $\Delta R(j, \gamma) > 0.3$. The scalar p_T sum of the jets and the photon, denoted S_T , reflects the visible energy scale of the event and is required to be larger than 300 GeV. Significant mismeasurement of jet p_T can lead to high p_T^{miss} , which is generally aligned with the mismeasured jet. To suppress such events, we require $\Delta\phi(\vec{p}_T^{\text{jet}}, \vec{p}_T^{\text{miss}}) > 0.3$ for the two highest p_T jets in the event. As the final state targeted contains only photons and hadronic jets, events with isolated electron and muon candidates are rejected to suppress the SM background arising from leptonic W decays. Further, events with an isolated leptonic or hadronic track are rejected, eliminating an additional $\approx 40\%$ of the relevant SM background processes. The event samples used for estimation of backgrounds are referred to as control regions (CRs) and are defined to be nonoverlapping with the baseline selection. These

| | |
|---|----------------------------------|
| p_T^{miss} [GeV] | > 300 GeV |
| N_{jets} ($p_T > 30$ GeV, $ \eta < 2.4$) | ≥ 2 |
| γ ($p_T > 100$ GeV, $ \eta < 2.4$) | ≥ 1 |
| $S_T = \sum_{\text{jets}} p_T + p_T^\gamma$ [GeV] | > 300 GeV |
| $\Delta\phi(\vec{p}_T^{\text{jet}}, \vec{p}_T^{\text{miss}})$ | > 0.3 for two highest p_T jets |
| Number of leptons (e, μ) | = 0 |
| Number of isolated tracks | = 0 |

Table 1. Summary of the baseline selection criteria used to identify events of interest for this search.

are designed — based on the presence of leptons (e or μ), lower p_T^{miss} values, or lower $\Delta\phi(\vec{p}_T^{\text{jet}}, \vec{p}_T^{\text{miss}})$ values — to be dominated by SM processes and are expected to have small signal contributions.

The events satisfying the baseline criteria are further classified into mutually exclusive signal regions (SRs) to enhance the sensitivity of the analysis to different signal scenarios. We define two sets of SRs called the electroweak (EW) and strong production (SP) SRs to target different types of signal models. The EW SRs include events with $2 \leq N_{\text{jets}} \leq 6$ and at least one V- or H-tag. These SRs are sensitive to electroweakino models like TChiWG, in which an energetic W, Z, or Higgs boson is expected in addition to low N_{jets} . They are also sensitive to gluino production models like T5qqqqZg in scenarios in which the difference between the masses of the gluino and the NLSP is small, resulting in soft jets and a boosted massive vector boson. The SP SRs include all baseline events not satisfying the EW SR selection criteria and are sensitive to gluino and squark pair production.

Both the SP and EW SRs are binned in p_T^{miss} , with lower bin edges of 300, 370, 450, 600, 750, and 900 GeV. These bins are chosen to ensure that each has an appreciable number of expected SM background events. For the SP SRs, each of the p_T^{miss} bins is further divided into bins of $N_{\text{jets}} = 2\text{--}4$, $5\text{--}6$, and ≥ 7 , and $N_{\text{b-tags}} = 0$ and ≥ 1 , where $N_{\text{b-tags}}$ is defined as the number of b-tagged jets in the event. For events with $N_{\text{b-tags}} = 0$ and $N_{\text{jets}} = 5\text{--}6$, the two highest p_T^{miss} bins are combined. For events with $N_{\text{b-tags}} = 0$ and $N_{\text{jets}} \geq 7$, and for all events with $N_{\text{b-tags}} \geq 1$, the three highest p_T^{miss} bins are combined. The EW p_T^{miss} bins are defined based on the presence of a V- or H-tag. This scheme results in a total of 27 SP and 10 EW SRs, all statistically independent. In addition, eight low- p_T^{miss} CRs are defined with $200 < p_T^{\text{miss}} < 300$ GeV in the aforementioned bins of N_{jets} and $N_{\text{b-tags}}$, or V- and H-tags, to be used for estimating the QCD multijet background. The definitions of all the SP and EW SRs and the low- p_T^{miss} CRs are summarized in figure 3. The indexing scheme shown in figure 3, with bin indices ranging from 1–45, is used to identify the SRs and low- p_T^{miss} CRs in the results presented in the following sections. The other CRs are explained in more detail in section 5.

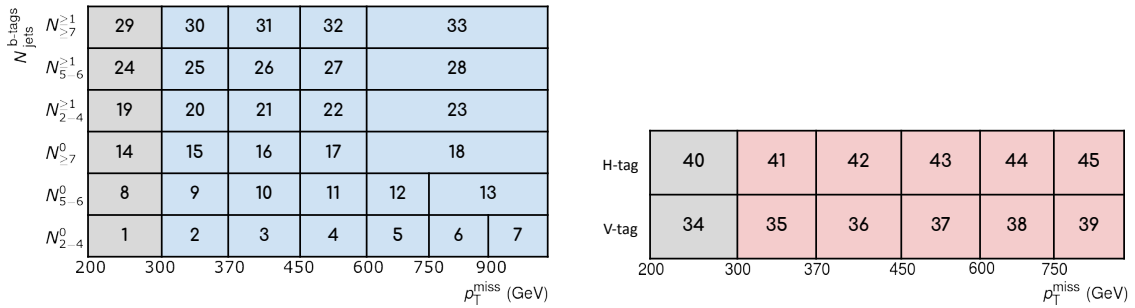


Figure 3. The definitions and indexing schemes for the SP (left) and EW (right) SRs and low- p_T^{miss} CRs, in the planes of p_T^{miss} , N_{jets} , and $N_{\text{b-tags}}$ (left) and p_T^{miss} , V- and H-tag (right). The gray blocks correspond to the low- p_T^{miss} CRs, the blue blocks to the SP SRs, and the red blocks to the EW SRs.

5 Background estimation

There are several SM processes that can result in final states containing at least one high- p_T photon, p_T^{miss} , and multiple jets. The production of $W\gamma+\text{jets}$, $t\bar{t}\gamma+\text{jets}$, $W+\text{jets}$, $t\bar{t}+\text{jets}$, $Z\gamma+\text{jets}$, $\gamma+\text{jets}$, and QCD multijet events are all non-negligible backgrounds for this search. The $W\gamma+\text{jets}$ and $t\bar{t}\gamma+\text{jets}$ events, with a prompt photon and a $W \rightarrow \ell' v$ ($\ell' = e, \mu$, and τ leptons) decay, enter the search regions as the “lost-lepton background” if the e or μ leptons are not identified, and therefore cannot be vetoed, or the τ leptons decay hadronically (τ_h). The $W+\text{jets}$ and $t\bar{t}+\text{jets}$ events contribute to the background if an electron originating from a W boson decay is misidentified as a photon. The $Z\gamma+\text{jets}$ process, with $Z \rightarrow vv$, is an irreducible background to this search. In all these processes, the presence of one or more neutrinos in the final states is the main source of p_T^{miss} . In $\gamma+\text{jets}$ events, a p_T mismeasurement of one or more jets can lead to large p_T^{miss} in the reconstructed events. The QCD multijet background arises similarly from artificial p_T^{miss} because of mismeasurement, but also requires that a jet be misidentified as a photon.

5.1 Lost-lepton background

An e or a μ is considered “lost” when it fails reconstruction, identification, or isolation, or if it is outside the detector or kinematic acceptance, as described in section 2. Events containing a τ_h candidate that is not rejected by the isolated track veto also contribute to the background, as the τ_h candidate is reconstructed as a jet. We estimate both these contributions together as the lost-lepton background, given their similar origins. The CRs used to estimate this background are collected by the same p_T^{miss} triggers as used for the SR events. There is one CR corresponding to each SR. Except the e , μ , and isolated track veto, the CRs are required to satisfy all criteria used to define the SRs. Instead, we require the presence of exactly one electron or one muon, and no additional isolated tracks in the event. It is important to note explicitly that these CR events are required to have a reconstructed photon in the final state. We require $m_T(p_T^\ell, p_T^{\text{miss}}) < 100$ GeV to veto events potentially arising from new physics in similar single-lepton final states. The relative composition of $W\gamma+\text{jets}$ and $t\bar{t}\gamma+\text{jets}$ events in the single- e and single- μ CRs, in

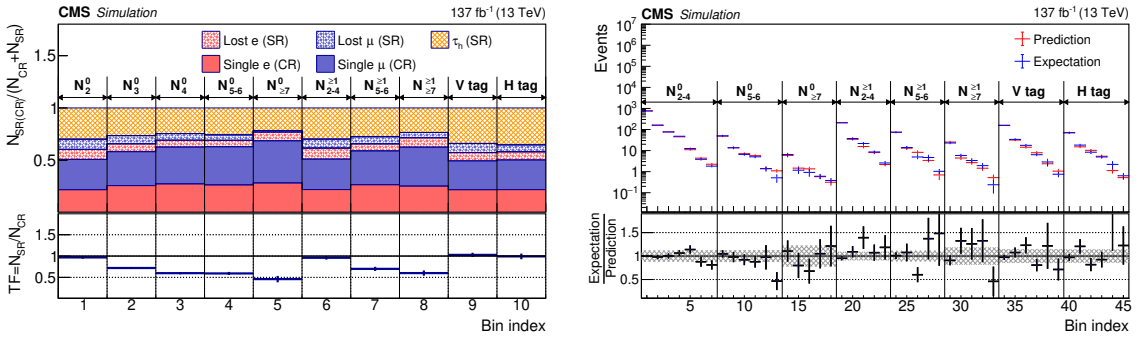


Figure 4. Left: the relative contributions of events with light lepton(s) or τ_h candidate(s) in the SRs and CRs (upper panel), and the corresponding transfer factors (TFs; see text), along with their statistical uncertainties (lower panel). Right: a comparison between the expected and predicted lost lepton event yields from simulated $W\gamma+jets$ and $t\bar{t}\gamma+jets$ processes in each of the SR bins. The vertical error bars indicate the statistical uncertainty in the simulation and the hashed bands in the lower panel indicate the systematic uncertainties.

the bins of N_{jets} and $N_{\text{b-tags}}$ for SP SRs and V- and H-tags for EW SRs, is shown in figure 4 (left). The SR events are shown as events containing a lost e, a lost μ , or a τ_h candidate. Since we do not use a dedicated τ_h veto, the last type of events are a large fraction of the lost-lepton background for this search.

The background estimation makes use of transfer factors (TFs) from the simulation. The TFs are defined as the ratio of the number of events in the SRs to the number of events in the respective CRs. The simulated event yields are corrected for known differences with data in lepton identification, b tagging, and trigger efficiency. The TFs are calculated in the bins of N_{jets} and $N_{\text{b-tags}}$ for the SP SRs and in the bins of V- and H-tag for the EW SRs; they are not binned in p_T^{miss} and include events with $p_T^{\text{miss}} > 200 \text{ GeV}$. The number of events predicted in SR bin i , $N_{0\ell\gamma}^{\text{data}}(i)$, is obtained from the number of events in the corresponding CR, $N_{1\ell\gamma}^{\text{data}}(i)$, as

$$N_{0\ell\gamma}^{\text{data}}(i) = \text{TF}(N_{\text{jets}}, N_{\text{b-tags}} \text{ or V-tag, H-tag}) N_{1\ell\gamma}^{\text{data}}(i). \quad (5.1)$$

Here, the TFs are applied to the single e and μ data CRs as per-event weights, depending on the event characteristics in terms of N_{jets} and $N_{\text{b-tags}}$ for the SP SRs and V- or H-tag for the EW SRs. As shown in the lower panel of figure 4 (left), these TFs vary from 0.5 to 1.0, depending on the SR.

We validate the background estimation method and the applicability of these TFs in the simulation by using the 1e γ and 1μ γ CRs to predict the events in the SRs using eq. (5.1). Comparisons of the expected and predicted event yields in the SRs are presented in figure 4 (right). The discrepancies between the expected and predicted yields, especially in the high p_T^{miss} or high N_{jets} bins, are covered by the statistical uncertainties.

The predicted number of lost-lepton background events can be affected by several sources of uncertainty that impact the TFs. To account for potential mismodeling of collinear photon radiation from quarks and leptons, the cross sections of relevant simulated

samples are varied by 20% [65] to account for differences in the modeling of photon radiation in different simulated samples and the effect on the TFs is found to be 4%. The uncertainty in the PDFs is evaluated by varying event weights from 100 PDF replicas [50, 51], resulting in a 3% effect. To evaluate the renormalization (μ_R) and factorization (μ_F) scale uncertainties, different weights obtained by varying the scales independently by 0.5 and 2 [66, 67] are used. The effect of this uncertainty is found to be 2% on the predicted number of lost-lepton background events. The uncertainties in the corrections applied to the simulation are propagated by varying their values and recalculating the predicted event yields in each SR. The variation in the number of predicted event yields with respect to the central values is taken as the respective uncertainty for each correction. The uncertainties in the lepton identification efficiency, b tagging efficiency, and the JEC and JER lead to 0.6, 0.7, 6, and 6% uncertainties in the lost-lepton background, respectively. The limited size of the simulated samples results in a 2–10% uncertainty in the predicted event yields. The estimated numbers of lost-lepton background events in each SR, along with uncertainties, are shown in section 7.

5.2 Misidentification of electrons as photons

If the track associated with an electron is not reconstructed or linked to it, the energy deposited by the electron in the ECAL could potentially be misidentified as a photon. Such electrons typically arise from $W+jets$, $t\bar{t}+jets$, and single top quark events in which a W boson decays to an electron and a neutrino. To estimate the background from electrons misidentified as photons, CRs are defined to include events containing exactly one electron with $p_T > 100$ GeV and zero photons satisfying the criteria described in section 2. Similar to the lost-lepton CRs, we require the m_T of the electron and p_T^{miss} to be < 100 GeV. Jets that have $\Delta R < 0.3$ with respect to the selected electron are not considered when computing S_T and N_{jets} .

The misidentification rate, f , is defined as the ratio of the number of events with a misidentified electron to the number of single-electron events. The rate f is determined using a sample of simulated $W+jets$ and $t\bar{t}+jets$ events containing $W \rightarrow e\nu$ decays. It depends on the kinematic properties of the electron and the presence of jets and other particles near the electron. The activity around the electron is characterized using the charged multiplicity, denoted Q_{mult} and defined as the number of charged constituents of the closest jet to the electron or photon with $\Delta R(\text{jet}, e \text{ or } \gamma) < 0.3$.

A correction factor α is included to account for differences in the rate f between data and simulation. The factor α is obtained from data and simulated events containing an e^+e^- pair with the “tag and probe” method [68]. The tag electron is required to have $p_T > 40$ GeV and to match within $\Delta R < 0.2$ with a generator-level electron arising from a Z boson in simulation or a trigger-level electron object in data. The probe electron (photon) is selected with requirements similar to the electron in the 1e CR (SR). The pair of the tag electron and the probe electron or photon is also required to satisfy $\Delta R(\text{tag}, \text{probe}) > 0.2$ and to have an invariant mass within 80–100 GeV. In this case, the rate f is defined as the ratio of the number of events with a photon as the probe to the number of events with an electron as the probe. The factor α is determined as the ratio of the rate f measured in data and simulated events, evaluated separately for events with $N_{\text{b-tags}} = 0$ and ≥ 1 .

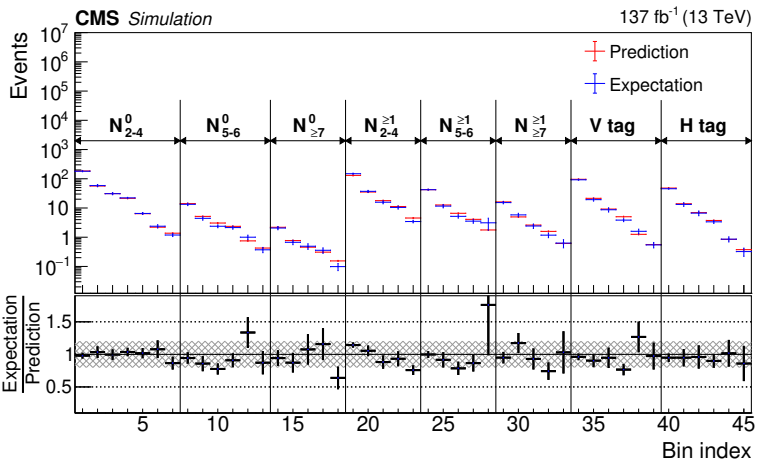


Figure 5. A comparison of the number of events with an electron misidentified as a photon in the SRs and the number estimated using the single-electron CRs with simulated samples. The ratio of the expected and predicted event yields in each SR is shown in the lower panel. The shaded region in the lower panel indicates the systematic uncertainties in the predicted number of background events.

To account for different run conditions, the factor α is also measured separately for data recorded in 2016, 2017, and 2018. The values of α vary from 1.9–2.4.

The number of events with the electrons misidentified as photons in the SR bin i , $N_\gamma^{\text{data}}(i)$, is estimated from the number of events in the corresponding CR, $N_{1e0\gamma}^{\text{data}}(i)$, as

$$N_\gamma^{\text{data}}(i) = f(p_T^e, Q_{\text{mult}}) \alpha(N_{\text{b-tags}}) N_{1e0\gamma}^{\text{data}}(i). \quad (5.2)$$

For a given CR, the rate f is applied as a per-event weight according to the p_T of the electron and the value of Q_{mult} for the jet closest to the electron. A comparison of the number of events expected in the SRs and predicted by the single-electron CRs, with both the SRs and CRs taken from simulated W+jets and t̄t+jets events, is shown in figure 5.

The uncertainties in the b tagging efficiencies, JECs, and JER smearing are propagated to the simulated events used to determine the rate f , and their effects on the final predicted event yields are found to be <1, 3, and 4%, respectively. The overall systematic uncertainty in α from topological differences in Z(ee) compared to t̄t and W+jets is estimated to be 20%, based on comparing simulated f values in e^+e^- events for the tag-and-probe and single-electron or single-photon selections. This component dominates the total systematic uncertainty in the predicted number of events with electrons misidentified as photons and is taken to be correlated across all SR bins. The uncertainties arising from the limited number of CR and SR events in the simulated samples are up to 20%. The statistical uncertainty in the single-electron CR in data contributes up to a 20% uncertainty in the predicted number of background events in the SRs. The background prediction in the SRs, along with the uncertainties, is shown in section 7.

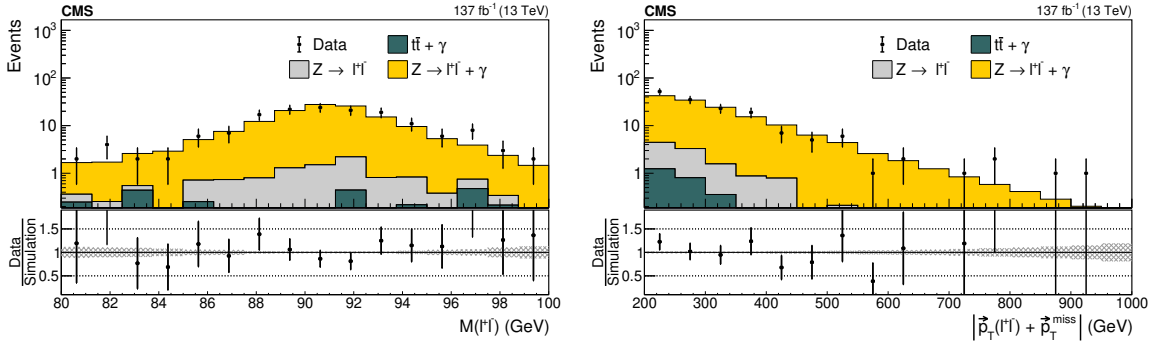


Figure 6. The distributions of the dilepton invariant mass (left) and the magnitude of the dilepton \vec{p}_T plus the \vec{p}_T^{miss} (right) for $\ell\ell\gamma$ events in data and simulation. The error bars represent the statistical uncertainty in the data events. In the lower panel, the shaded region shows the statistical uncertainty in the simulation.

5.3 $Z(vv)\gamma+\text{jets}$ background

The presence of energetic neutrinos in $Z(vv)\gamma+\text{jets}$ events manifests as large p_T^{miss} and results in significant background for searches in final states requiring zero leptons, particularly in low- N_{jets} and high- p_T^{miss} SRs. We use $Z(vv)\gamma+\text{jets}$ simulated events to estimate the predicted event yields in the SP SRs, which are defined by N_{jets} , $N_{\text{b-tags}}$, and p_T^{miss} . These event yields are adjusted by the ratio of the number of $Z(\text{ee})\gamma+\text{jets}$ and $Z(\mu\mu)\gamma+\text{jets}$ events, collectively called $Z(\ell\ell)\gamma$ events, measured in data and simulation to account for any potential mismodeling of $Z\gamma+\text{jets}$ production. The leptonic final states of Z boson decays have limited numbers of events because of their small branching fractions and hence are not directly used to estimate the $Z(vv)\gamma+\text{jets}$ background.

To select $Z(\ell\ell)\gamma$ events, we require a pair of light leptons with the same flavor, opposite charge, and invariant mass in the range of 80–100 GeV, depicted in figure 6 (left). The p_T^{miss} in these events is required to be less than 200 GeV. However, to mimic the kinematic properties of the $Z(vv)$ process in the SRs, the dilepton system should be treated as invisible. Therefore, the magnitude of the sum of the dilepton \vec{p}_T and the \vec{p}_T^{miss} , shown in figure 6 (right), must be greater than 300 GeV, following the baseline selection. We also require $\Delta R(\ell, \gamma) > 0.2$ to ensure that the photon is not radiated from one of the leptons. The numbers of events obtained in data and simulation using these criteria are denoted $N_{\ell\ell\gamma}^{\text{data}}$ and $N_{\ell\ell\gamma}^{\text{MC}}$, respectively. Here, the subscript ℓ refers to electrons and muons.

The number of events in the SRs is obtained using the expression:

$$N_{Z(vv)\gamma}^{\text{data}}(i) = \left(\frac{N_{\ell\ell\gamma}^{\text{data}} \beta_{\ell\ell\gamma}}{N_{\ell\ell\gamma}^{\text{MC}}} \right)_j N_{Z(vv)\gamma}^{\text{MC}}(i), \quad (5.3)$$

where $N_{Z(vv)\gamma}^{\text{data}}(i)$ and $N_{Z(vv)\gamma}^{\text{MC}}(i)$ are the numbers of events predicted in SR i in data and simulation, respectively, and $\beta_{\ell\ell\gamma} = 1 - N_{t\bar{t}\gamma}/N_{\ell\ell\gamma}$ is a correction factor to account for the contribution of $t\bar{t}\gamma+\text{jets}$ processes to the $\ell\ell\gamma$ events in data. The index $j = 0$ or 1 corresponds to $N_{\text{b-tags}} = 0$ or ≥ 1 . The contribution of $t\bar{t}\gamma$ is estimated from simulation and it is found to be statistically compatible with the number of opposite-sign, different-flavor

$(e^\pm \mu^\mp)$ events from data. As the contamination of $t\bar{t}\gamma$ events is expected to be higher in the SRs with $N_{b\text{-tags}} \geq 1$, the factor $\beta_{\ell\ell\gamma}$ is derived separately for the regions with and without a b-tagged jet.

The corrections to $Z(vv)\gamma + \text{jets}$ events from $\ell\ell\gamma$ events are 1.07 ± 0.09 and 1.01 ± 0.28 for $N_{b\text{-tags}} = 0$ and ≥ 1 , respectively. These uncertainties are propagated to the predicted number of events in the SRs along with the statistical uncertainty in the $Z(vv)\gamma + \text{jets}$ simulated samples, which ranges from 2–70%. In both the SP and EW SRs, the statistical uncertainty is larger in the high- p_T^{miss} bins. To account for any mismodeling of photon p_T in the simulation, we apply an additional systematic uncertainty, which ranges 18–40%, depending on the p_T^{miss} bin. This is assessed based on the results presented in ref. [69]. The number of $Z(vv)\gamma + \text{jets}$ events for each SR, along with the uncertainty in the prediction, is presented in section 7.

5.4 $\gamma + \text{jets}$ and QCD multijet background

QCD multijet and $\gamma + \text{jets}$ events with a well-reconstructed photon can contribute to the SRs if they also contain large p_T^{miss} resulting from significant mismeasurement of one or more jets or from the presence of neutrinos from the semileptonic decays of heavy-flavor hadrons. We use an “ABCD” method to estimate this background, where the regions A, B, and C are data CRs designed to be nonoverlapping with the SRs and the region D corresponds to the SRs. To define these CRs, we use events with $200 < p_T^{\text{miss}} < 300 \text{ GeV}$ (low- p_T^{miss}) or $\Delta\phi(p_T^{\text{jet}}, p_T^{\text{miss}}) < 0.3$, indicating at least one of the two leading jets is aligned with the direction of p_T^{miss} (low- $\Delta\phi$). These events are required to satisfy all other baseline selection criteria. From the observed event yields in every CR, we subtract the contributions from the lost-lepton, misidentified electron, and $Z\gamma + \text{jets}$ backgrounds, which are obtained using the same methods as used for the SRs.

The CRs A and C consist of events with low- p_T^{miss} , with the former being low- $\Delta\phi$ and the latter being high- $\Delta\phi$. These events are divided into the same exclusive regions based on N_{jets} , $N_{b\text{-tags}}$, V- and H-tag as used to define the SP and EW SRs. In each of these regions, a ratio $R_{\text{low-}p_T^{\text{miss}}}$ is defined as the number of events with high- $\Delta\phi$ (CR C) to that with low- $\Delta\phi$ (CR A). The CR B consists of events with high- p_T^{miss} and low- $\Delta\phi$. These events are divided into the same regions as the SRs, including the p_T^{miss} binning. The predicted number of events in SR i is then:

$$N_{\text{multijet}+\gamma}^{\text{data}}(i) = R_{\text{low-}p_T^{\text{miss}}}(r)\kappa(r)N_B^{\text{data}}(i), \quad (5.4)$$

where the index i refers to the SR and the index r refers to the bins defined based on N_{jets} , $N_{b\text{-tags}}$, V-tag, and H-tag as used for the SRs. The factor $\kappa(r)$ is used as a correction determined from the simulation to account for any differences in the ratios of the low- p_T^{miss} regions A and C compared to the high- p_T^{miss} regions B and D. It is calculated in the same bins as used for $R_{\text{low-}p_T^{\text{miss}}}$ as

$$\kappa(r) = \frac{R_{\text{high-}p_T^{\text{miss}}}(r)}{R_{\text{low-}p_T^{\text{miss}}}(r)}. \quad (5.5)$$

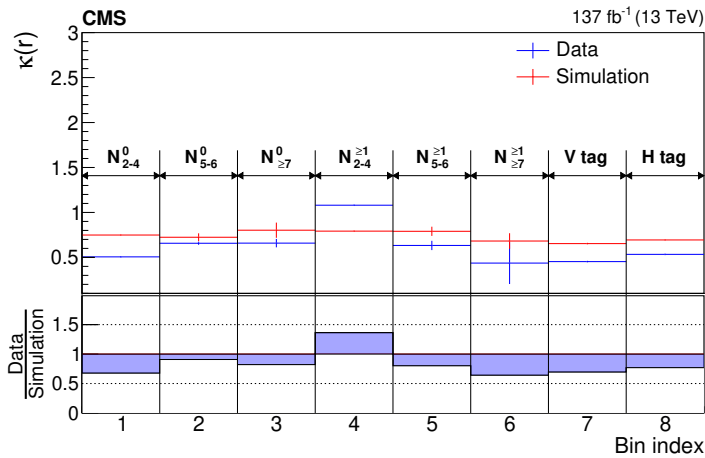


Figure 7. A comparison between κ estimated from simulation and from data in the zero-photon CR. The values are given for each N_{jets} , $N_{\text{b-tags}}$, V-tag, and H-tag bin, represented as r . The blue bands in the lower panel represent the relative systematic uncertainty in κ .

This method is validated in the simulation. The CRs and SRs are defined using the simulated γ +jets and QCD multijet events. The same event sample is also used to measure $R_{\text{low-}p_{\text{T}}^{\text{miss}}}$. The numbers of events predicted by the method in various SRs are found to be consistent with the expected values, within the statistical precision. The test of the method in simulation is nontrivial because the parametrization of κ is based on N_{jets} , $N_{\text{b-tags}}$, V- and H-tag bins, whereas the predictions are done for each of the SRs, which also include $p_{\text{T}}^{\text{miss}}$ binning.

Since κ is an important ingredient for this background estimation and it is obtained from the simulation, we validate these factors in data and simulation samples using events that do not contain a photon, referred to as zero-photon events. The zero-photon region is dominated by multijet events. The contributions from the other SM background processes are small, so they are estimated from the simulation and subtracted from the zero-photon event yields. The values of κ derived from data and simulation differ by 10–36%, as shown in figure 7. The observed differences are treated as systematic uncertainties in the predicted number of events. There is one κ value for each set of N_{jets} , $N_{\text{b-tags}}$, V-tag, and H-tag requirements, so the uncertainty in κ is correlated among all the corresponding SRs. The statistical uncertainties in κ and the number of events in low- $p_{\text{T}}^{\text{miss}}$ regions vary in the range 10–50%. Section 7 summarizes the predicted number of γ +jets and QCD multijet events in the SRs.

6 Systematic uncertainties

The sources of systematic uncertainty and their effects on the predicted numbers of events for the lost-lepton, electron misidentified as photon, Z(vv)+jets, and γ +jets backgrounds have been discussed in section 5. The following sources of systematic uncertainty are considered for the simulated signal event yields. The uncertainties in the total integrated

luminosity [70–72] affect the signal yield in each SR. This effect is taken to be 1.6% for all the SRs and all signal models. The uncertainties in the JEC and JER measurements from data are propagated to individual jets, and their effect on event yields is taken as an uncertainty in the respective SR bins. The effect of variations in the pileup reweighting is estimated in a similar way. The uncertainties related to pileup, JECs, and JER contribute approximately 2% each. The uncertainty in the trigger efficiency for simulated signal events varies from 3–10%, with larger values for SRs with lower p_T^{miss} . The uncertainties related to the isolated track veto and jet ID modeling in the fast simulation are 2 and 1%, respectively. The b tagging efficiency and light flavor quark mistagging rates in the fast simulation signal samples are corrected with factors derived from the GEANT4-based simulation and data. The uncertainties in these corrections are propagated to the final signal yield, and their effect in the SP SRs is up to 10%. The statistical uncertainty from the limited number of simulated events in the signal samples ranges 0.7–38% when considering all bins; when considering only the most sensitive bins, this uncertainty decreases to 0.1–7%.

The PDF uncertainty, and the μ_R and μ_F scale uncertainties that affect the total production cross section are treated as theoretical uncertainties. The effects of these on the signal yield are 2 and 5%, respectively. The modeling of initial-state radiation (ISR) in the signal simulation is corrected by applying data-to-simulation correction factors [73]. The corrections depend on the number of ISR jets and the p_T of the chargino-neutralino system for the strong production and the electroweak signal models, respectively. These uncertainties have magnitudes of 25% for strong production and 10% for electroweak signal models. Table 2 summarizes the sources of systematic uncertainty and their effects on the predicted backgrounds and signal yields.

7 Results and interpretation

We perform a simultaneous maximum likelihood fit to the number of events in the low- and high- $\Delta\phi$ regions to predict the number of SM background events in the SRs. The profile likelihood ratio q_μ is used as the test statistic to compute limits in the modified frequentist CL_s approach [74, 75], employing the asymptotic approximation [76]. The statistic is defined as $q_\mu = -2 \ln(\mathcal{L}_\mu / \mathcal{L}_{\max})$, where μ is the SUSY signal strength, \mathcal{L}_{\max} is the maximum likelihood from varying all parameters including μ , and \mathcal{L}_μ is the maximum likelihood for a fixed μ . The observed numbers of events in various CRs are modeled using gamma distributions, which correctly represent the statistical uncertainties. The predicted yield of signal events in each CR is found to be negligible. The other systematic uncertainties listed in table 2 are modeled as log-normal constraints in the likelihood. The results obtained from the CR-only fit under the background-only hypothesis are shown in figure 8. The numerical values, including the uncertainties in each background prediction, are given in appendix A. In most of the SRs, the observed event yields are consistent with the predictions, indicating no significant presence of signal events. The maximum deviation observed is about 2 standard deviations below the prediction, in bin 13 ($5 \leq N_{\text{jets}} \leq 6$, $N_{\text{b-tags}} = 0$, $p_T^{\text{miss}} \geq 750 \text{ GeV}$), bin 16 ($N_{\text{jets}} \geq 7$, $N_{\text{b-tags}} = 0$, $370 < p_T^{\text{miss}} < 450 \text{ GeV}$), and bin 44 (H-tag, $600 < p_T^{\text{miss}} < 750 \text{ GeV}$).

| Source | Lost lepton | Misidentified e | $Z(vv)\gamma$ | Multijet+ γ | Signal |
|---|-------------|-----------------|---------------|--------------------|---------|
| Integrated luminosity | — | — | — | — | 1.6 |
| Limited number of CR events | 3–100 | 5–20 | 8–28 | 2–100 | — |
| Limited number of simulated events | 2–10 | 2–20 | 2–70 | 10–50 | 0.7–38 |
| b tagging | 0–1 | 0–1 | — | — | 0–10 |
| PDF | 3 | — | — | — | 1–2 |
| μ_R and μ_F scales | 2 | — | — | — | 0.3–5 |
| JEC | 0–6 | 0–3 | — | — | 1–2 |
| JER | 0–6 | 0–4 | — | — | 1–2 |
| Pileup | — | — | — | — | 0.1–0.3 |
| Trigger efficiency | — | — | — | — | 3–10 |
| Collinear γ | 4 | — | — | — | — |
| α | — | 20 | — | — | — |
| Modeling of γp_T | — | — | 18–40 | — | — |
| κ modeling | — | — | — | 10–36 | — |
| Stat. unc. in low- p_T^{miss} A, C regions | — | — | — | 10–50 | — |
| Isolated track veto | — | — | — | — | 2 |
| Jet ID | — | — | — | — | 1 |

Table 2. The systematic uncertainties in the predicted background and signal event yields (in %). A dash (—) indicates that the source of uncertainty is not applicable or negligible.

The measured backgrounds along with their uncertainties and the observed number of events in the SRs are used to determine 95% confidence level (CL) upper limits on the production cross sections of various SUSY models, discussed in section 1, using a maximum likelihood fit. We compare these upper limits with theoretical production cross sections, and determine lower limits on masses of the SUSY particles in specific models and final states, which are excluded by this search. The exclusion limits in terms of masses of particles involved in a given model are shown in figure 9 for gluino and squark pair production scenarios. Figure 10 presents the same for the production of electroweakino pairs.

For the gluino production model with a decay to $b\bar{b}$ and NLSP (T5bbbbZG), the observed (expected) gluino mass exclusion is up to 2.32 (2.27) TeV for small NLSP masses. In the T5qqqqHG and the T5ttttZG models, the observed (expected) upper limits on the gluino masses extend to 2.35 (2.30) and 2.26 (2.25) TeV, respectively. The mass limits degrade for very high and very low NLSP masses. When the NLSP masses are large, the p_T^{miss} is large but the events contain lower hadronic activity (N_{jets}). For the low NLSP masses, hadronic activity is high, but p_T^{miss} is low. In these scenarios, either the signal acceptance is low or the signals populate SRs with larger backgrounds, resulting in a decrease in the sensitivity of the analysis. These features are illustrated in the open histograms shown in figure 8. For the T5qqqqHG scenario, the observed limits are stronger than the expected ones because of the small deficit in the observed event yields in the high- N_{jets} and $N_{\text{b-tags}} = 0$ regions and in the high- p_T^{miss} H-tag regions. In the strong production models that involve

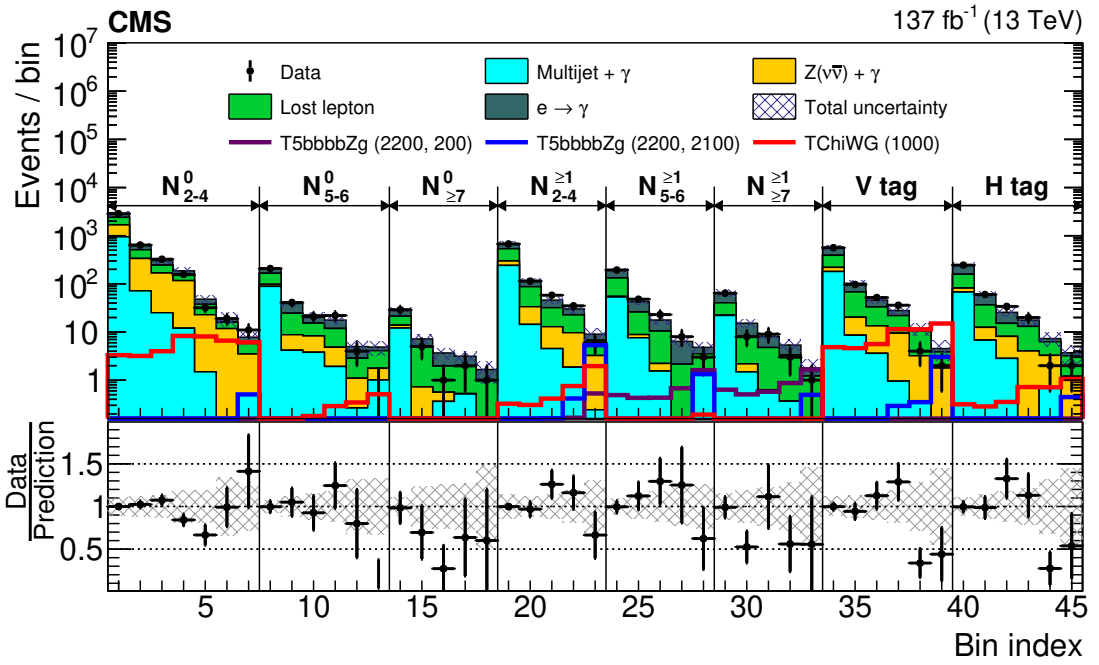


Figure 8. The numbers of predicted background events and observed events in the SRs and low- p_T^{miss} CRs. The lost-lepton, electron misidentified as photon, $Z\gamma$ +jets, and γ +jets and QCD multijet backgrounds are stacked histograms. The observed numbers of events in data are presented as black points. For illustration, the expected event yields are presented for the signal model T5bbbbZG, for small (blue) and large (purple) differences in the masses of the \tilde{g} and NLSP. Also shown is the expected distribution of events for the signal model TChiWG (red). The numerical values in parentheses in the legend entries for the signal models indicate the \tilde{g} and NLSP mass values in GeV for strong production and the NLSP mass value for electroweak production. The lower panel shows the ratio of the observed number of data events and the predicted backgrounds. The error bars represent the statistical uncertainty in the data events, and the shaded band represents the statistical and systematic uncertainties in the predicted background. The p_T^{miss} bin 200–300 GeV is used for the estimation of the γ +jets and QCD multijet background.

off-shell Z bosons and very low NLSP masses, the limits are stronger than those from on-shell Z bosons, because the former imparts larger p_T to the gravitinos, leading to larger p_T^{miss} . In the T5qqqqHG model, off-shell Higgs boson decays are not considered. For the top squark pair production model (T6ttZg), where the top squark decays into a top quark and NLSP, the expected mass limit is 1.38 TeV and the observed mass limit is 1.43 TeV. There is an approximately 0.7 standard deviation difference between the expected and observed limits, which comes from signal regions with high p_T^{miss} , high N_{jets} , and $N_{\text{b-tags}} \geq 1$.

In electroweak production models, for sufficiently large electroweakino masses, the signal events mostly populate large p_T^{miss} and V- or H-tag signal regions. In the TChiWG scenario, we observe (expect) the exclusion of $\tilde{\chi}_1^\pm \tilde{\chi}_1^0$ masses up to 1.23 (1.17) TeV, assuming wino-like $\tilde{\chi}_1^\pm \tilde{\chi}_1^0$ production. In the TChiNG model, the $\tilde{\chi}_1^\pm$, $\tilde{\chi}_1^0$, and $\tilde{\chi}_2^0$ are nearly mass degenerate, and we use higgsino-like cross sections to interpret the results. Electroweakino

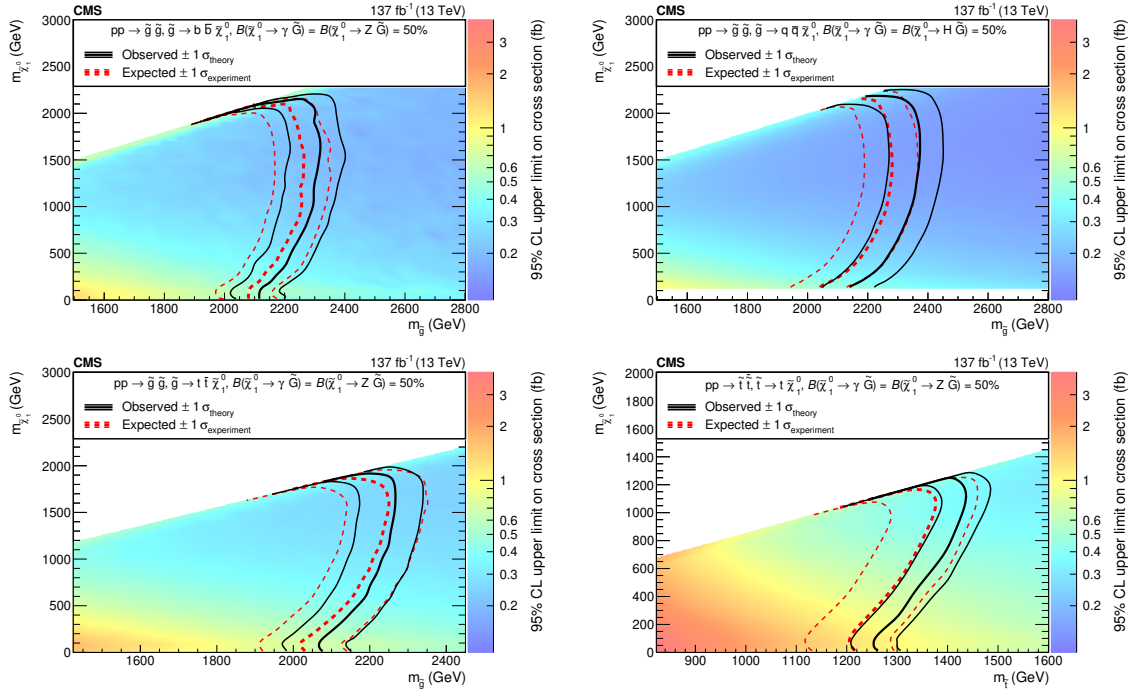


Figure 9. The 95% CL upper limits on the production cross sections for \tilde{g} pairs, with $\tilde{g} \rightarrow b\bar{b}\tilde{\chi}_1^0$ followed by $\tilde{\chi}_1^0 \rightarrow Z\tilde{G}$ or $\tilde{\chi}_1^0 \rightarrow \gamma\tilde{G}$ (upper left, T5bbbbZG model), $\tilde{g} \rightarrow q\bar{q}\tilde{\chi}_1^0$ followed by $\tilde{\chi}_1^0 \rightarrow H\tilde{G}$ or $\tilde{\chi}_1^0 \rightarrow \gamma\tilde{G}$ (upper right, T5qqqqHG model), $\tilde{g} \rightarrow t\bar{t}\tilde{\chi}_1^0$ followed by $\tilde{\chi}_1^0 \rightarrow Z\tilde{G}$ or $\tilde{\chi}_1^0 \rightarrow \gamma\tilde{G}$ (lower left, T5ttttZG model), or top squark pairs assuming the top squark decays to a top quark and a $\tilde{\chi}_1^0$ followed by $\tilde{\chi}_1^0 \rightarrow Z\tilde{G}$ or $\tilde{\chi}_1^0 \rightarrow \gamma\tilde{G}$ (lower right, T6tttZG model). The thick black curve represents the observed exclusion contour and the thin black curves show the effect of varying the signal cross section within the theoretical uncertainties by $\pm 1\sigma_{\text{theory}}$. The thick red curve indicates the expected exclusion contour and the thin red curves show the variations from $\pm 1\sigma_{\text{experiment}}$ uncertainties.

masses below 1.05 (0.95) TeV are observed (expected) to be excluded, assuming the $\tilde{\chi}_1^\pm$ and $\tilde{\chi}_2^0$ decays give rise to $\tilde{\chi}_1^0$ and soft particles. The expected upper limit on the mass is about 60–80 GeV smaller than the observed upper limit because of a deficit in the observed event yields in the highest p_T^{miss} bins of the V- and H-tag SRs. For the lower electroweakino masses, the signal populates moderate p_T^{miss} bins, which have observed event yields higher than the predictions by about one standard deviation. This leads to higher than predicted observed upper limits on the production cross section. Alternatively, if only the $\tilde{\chi}_1^0\tilde{\chi}_2^0$ process occurs in this model, there is no exclusion in the range of NLSP masses considered in this search, based on the theoretically predicted cross section. In the TChiNGnn model, with only the $\tilde{\chi}_1^0\tilde{\chi}_2^0$ process, the observed (expected) NLSP mass limit is 0.50 (0.65) TeV. The observed limit is weaker than expected because of upward fluctuations in several low- N_{jets} $N_{\text{b-tags}} \geq 1$, V-tag, and H-tag SR bins with intermediate p_T^{miss} values.

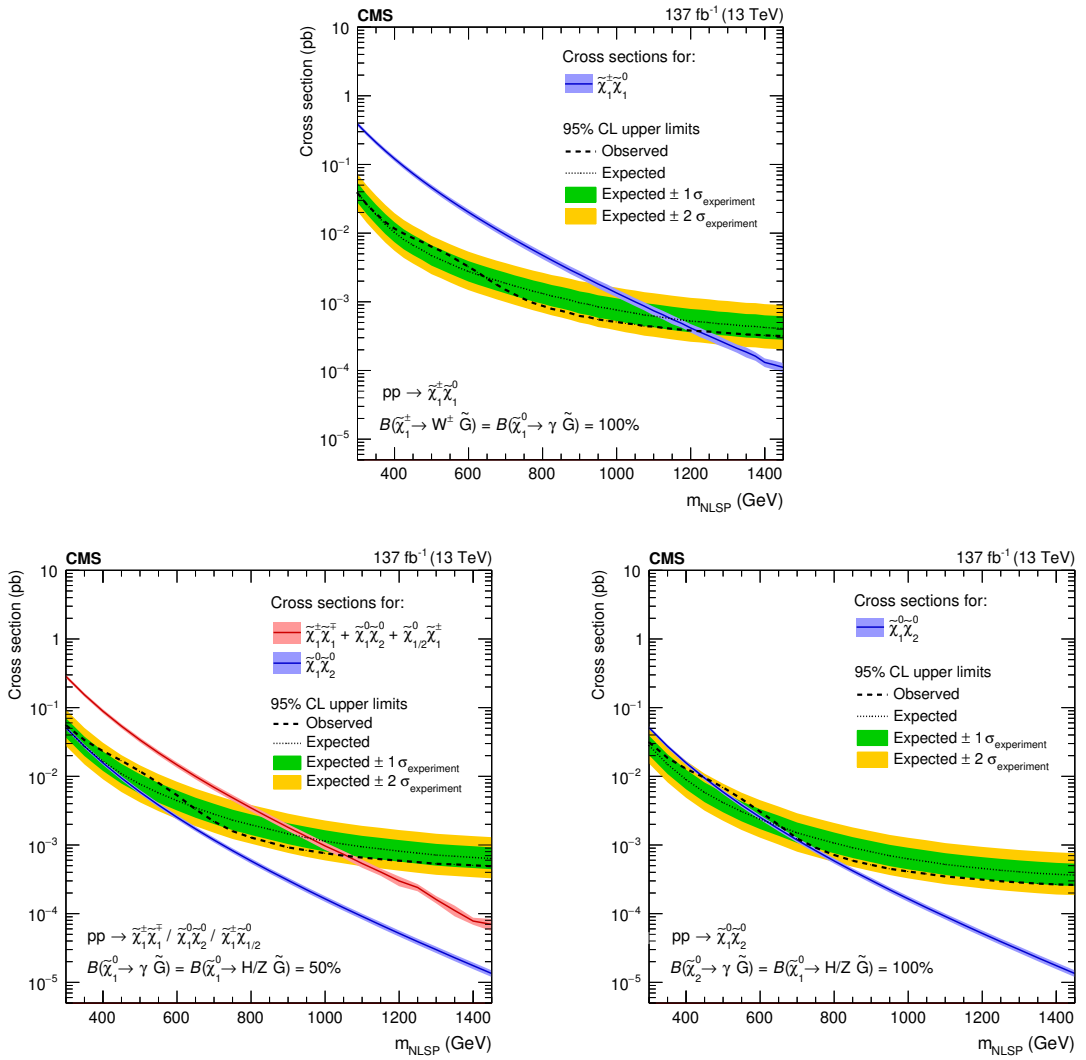


Figure 10. The expected and observed limits on the electroweakino mass in the TChiWG (upper), TChiNG (lower left), and TChiNGnn (lower right) models at 95% CL. For the TChiNG model (lower left), scenarios with degenerate charginos and neutralinos leading to the combined process $\tilde{\chi}_1^{\pm}\tilde{\chi}_1^{\mp} + \tilde{\chi}_1^0\tilde{\chi}_2^0 + (\tilde{\chi}_1^0/\tilde{\chi}_2^0)\tilde{\chi}_1^{\pm}$ (red) or the single process $\tilde{\chi}_1^0\tilde{\chi}_2^0$ (blue) are considered.

8 Summary

A search for supersymmetry (SUSY) is presented using events with final states containing at least one photon, large missing transverse momentum, and jets that may or may not arise from b quarks. These signatures are motivated by models with gauge-mediated SUSY breaking (GMSB), in which the lightest SUSY particle (LSP) is a gravitino (\tilde{G}) and the next-to-LSP (NLSP) is a chargino ($\tilde{\chi}_1^{\pm}$) or neutralino ($\tilde{\chi}_1^0$), collectively called electroweakinos. Several simplified models of strong production of pairs of gluinos (\tilde{g}) and top squarks (\tilde{t}) are considered, with the gluino decaying to a pair of quarks along with an NLSP or the top squark decaying to a top quark and an NLSP; the NLSP then

decays to a neutral gauge boson (photon, Z boson, or Higgs boson) and an LSP. Models of pair production of electroweakinos are also considered, with the neutralinos decaying as described above, and the charginos decaying to a W boson and an LSP.

Compared to previous searches, this search achieves increased sensitivity to scenarios with small mass differences between the gluino and the NLSP with dedicated search regions based on identifying boosted massive bosons. In addition, the search strategy is expanded to provide sensitivity to the production of electroweakino pairs. The observations are consistent with the standard model expectations and 95% confidence level upper limits are set on the production cross sections of SUSY particles. In the GMSB simplified models, the lower gluino mass limit reaches up to 2.35 TeV for models with $\tilde{g} \rightarrow q\bar{q}\tilde{\chi}_1^0$ followed by $\tilde{\chi}_1^0 \rightarrow H\tilde{G}$ or $\gamma\tilde{G}$ with equal probability, and the top squark mass limit reaches up to 1.43 TeV for models with $\tilde{t} \rightarrow t\tilde{\chi}_1^0$ followed by $\tilde{\chi}_1^0 \rightarrow Z\tilde{G}$ or $\gamma\tilde{G}$ with equal probability. These results extend the previous mass limits [27] on gluinos and top squarks by 150–200 GeV. For electroweakino pair production, chargino and neutralino masses up to 1.23 TeV are excluded, assuming wino-like electroweakinos with decays $\tilde{\chi}_1^\pm \rightarrow W\tilde{G}$ and $\tilde{\chi}_1^0 \rightarrow \gamma\tilde{G}$. The higgsino-like electroweakino mass limits reach up to 1.05 TeV for models with $\tilde{\chi}_1^0 \rightarrow \gamma\tilde{G}$, $Z\tilde{G}$, or $H\tilde{G}$ with 50, 25, and 25% branching fractions, respectively. These are the best mass limits to date on electroweakino production with photons in the final state.

Acknowledgments

We congratulate our colleagues in the CERN accelerator departments for the excellent performance of the LHC and thank the technical and administrative staffs at CERN and at other CMS institutes for their contributions to the success of the CMS effort. In addition, we gratefully acknowledge the computing centres and personnel of the Worldwide LHC Computing Grid and other centres for delivering so effectively the computing infrastructure essential to our analyses. Finally, we acknowledge the enduring support for the construction and operation of the LHC, the CMS detector, and the supporting computing infrastructure provided by the following funding agencies: SC (Armenia), BMBWF and FWF (Austria); FNRS and FWO (Belgium); CNPq, CAPES, FAPERJ, FAPERGS, and FAPESP (Brazil); MES and BNSF (Bulgaria); CERN; CAS, MoST, and NSFC (China); MINCIENCIAS (Colombia); MSES and CSF (Croatia); RIF (Cyprus); SENESCYT (Ecuador); MoER, ERC PUT and ERDF (Estonia); Academy of Finland, MEC, and HIP (Finland); CEA and CNRS/IN2P3 (France); BMBF, DFG, and HGF (Germany); GSRI (Greece); NKFIH (Hungary); DAE and DST (India); IPM (Iran); SFI (Ireland); INFN (Italy); MSIP and NRF (Republic of Korea); MES (Latvia); LAS (Lithuania); MOE and UM (Malaysia); BUAP, CINVESTAV, CONACYT, LNS, SEP, and UASLP-FAI (Mexico); MOS (Montenegro); MBIE (New Zealand); PAEC (Pakistan); MES and NSC (Poland); FCT (Portugal); MESTD (Serbia); MCIN/AEI and PCTI (Spain); MOSTR (Sri Lanka); Swiss Funding Agencies (Switzerland); MST (Taipei); MHESI and NSTDA (Thailand); TUBITAK and TENMAK (Turkey); NASU (Ukraine); STFC (United Kingdom); DOE and NSF (U.S.A.).

Individuals have received support from the Marie-Curie programme and the European Research Council and Horizon 2020 Grant, contract Nos. 675440, 724704, 752730, 758316,

765710, 824093, 884104, and COST Action CA16108 (European Union); the Leventis Foundation; the Alfred P. Sloan Foundation; the Alexander von Humboldt Foundation; the Science Committee, project no. 22rl-037 (Armenia); the Belgian Federal Science Policy Office; the Fonds pour la Formation à la Recherche dans l’Industrie et dans l’Agriculture (FRIA-Belgium); the Agentschap voor Innovatie door Wetenschap en Technologie (IWT-Belgium); the F.R.S.-FNRS and FWO (Belgium) under the “Excellence of Science — EOS” — be.h project n. 30820817; the Beijing Municipal Science & Technology Commission, No. Z191100007219010; the Ministry of Education, Youth and Sports (MEYS) of the Czech Republic; the Shota Rustaveli National Science Foundation, grant FR-22-985 (Georgia); the Deutsche Forschungsgemeinschaft (DFG), under Germany’s Excellence Strategy — EXC 2121 “Quantum Universe” — 390833306, and under project number 400140256 — GRK2497; the Hellenic Foundation for Research and Innovation (HFRI), Project Number 2288 (Greece); the Hungarian Academy of Sciences, the New National Excellence Program — ÚNKP, the NKFIH research grants K 124845, K 124850, K 128713, K 128786, K 129058, K 131991, K 133046, K 138136, K 143460, K 143477, 2020-2.2.1-ED-2021-00181, and TKP2021-NKTA-64 (Hungary); the Council of Science and Industrial Research, India; the Latvian Council of Science; the Ministry of Education and Science, project no. 2022/WK/14, and the National Science Center, contracts Opus 2021/41/B/ST2/01369 and 2021/43/B/ST2/01552 (Poland); the Fundação para a Ciência e a Tecnologia, grant CEECIND/01334/2018 (Portugal); the National Priorities Research Program by Qatar National Research Fund; MCIN/AEI/10.13039/501100011033, ERDF “a way of making Europe”, and the Programa Estatal de Fomento de la Investigación Científica y Técnica de Excelencia María de Maeztu, grant MDM-2017-0765 and Programa Severo Ochoa del Principado de Asturias (Spain); the Chulalongkorn Academic into Its 2nd Century Project Advancement Project, and the National Science, Research and Innovation Fund via the Program Management Unit for Human Resources & Institutional Development, Research and Innovation, grant B05F650021 (Thailand); the Kavli Foundation; the Nvidia Corporation; the SuperMicro Corporation; the Welch Foundation, contract C-1845; and the Weston Havens Foundation (U.S.A.).

A Predicted and observed events

In this appendix, we present the numerical values and uncertainties for each of the signal and low- p_T^{miss} regions defined in figure 3. These values correspond to the results presented in figure 8.

| p_T^{miss} | region [GeV] | Lost lepton | e misidentified as γ | Z(vv) γ | Multijet+ γ | Total pred. | Observed |
|---|-------------------|-------------------|-----------------------------|-----------------------|--------------------|-------------|----------|
| $2 \leq N_{\text{jets}} \leq 4, N_{\text{b-tags}} = 0$ | | | | | | | |
| 200–300 | 731 \pm 64 | 459 \pm 97 | 730 \pm 146 | 946 \pm 267 | 2870 \pm 317 | 2865 | |
| 300–370 | 174 \pm 19 | 116 \pm 26 | 265 \pm 59 | 71.5 \pm 25.8 | 626 \pm 72 | 641 | |
| 370–450 | 76.5 \pm 9.7 | 58.2 \pm 13.0 | 143 \pm 36 | 25.1 \pm 9.0 | 303 \pm 40 | 325 | |
| 450–600 | 33.1 \pm 5.5 | 36.5 \pm 7.7 | 105 \pm 34 | 12.0 \pm 4.3 | 186 \pm 36 | 157 | |
| 600–750 | 14.8 \pm 3.6 | 10.4 \pm 2.3 | 21.3 \pm 7.3 | 1.49 \pm 0.54 | 48.0 \pm 8.8 | 32 | |
| 750–900 | 4.17 \pm 1.65 | 3.23 \pm 0.72 | 11.8 \pm 6.4 | 0 \pm 0.00360 | 19.2 \pm 6.4 | 19 | |
| ≥ 900 | 2.59 \pm 1.33 | 1.71 \pm 0.50 | 3.00 \pm 1.73 | 0.491 \pm 0.177 | 7.79 \pm 2.16 | 11 | |
| $5 \leq N_{\text{jets}} \leq 6, N_{\text{b-tags}} = 0$ | | | | | | | |
| 200–300 | 68.3 \pm 8.0 | 42.7 \pm 9.5 | 8.96 \pm 2.62 | 88.6 \pm 7.8 | 209 \pm 14 | 208 | |
| 300–370 | 15.8 \pm 3.4 | 14.5 \pm 3.3 | 4.60 \pm 1.71 | 4.17 \pm 0.88 | 39.0 \pm 4.7 | 41 | |
| 370–450 | 7.00 \pm 2.24 | 7.39 \pm 1.63 | 4.49 \pm 1.85 | 3.79 \pm 0.80 | 22.7 \pm 3.3 | 21 | |
| 450–600 | 7.00 \pm 2.10 | 5.84 \pm 1.44 | 2.90 \pm 1.77 | 1.92 \pm 0.41 | 17.7 \pm 3.1 | 22 | |
| 600–750 | 1.75 \pm 1.10 | 2.15 \pm 0.54 | 0.831 \pm 1.009 | 0.264 \pm 0.056 | 5.00 \pm 1.61 | 4 | |
| ≥ 750 | 2.33 \pm 1.22 | 0.779 \pm 0.254 | 0.754 \pm 1.014 | 1.01 \pm 0.21 | 4.87 \pm 1.61 | 0 | |
| $N_{\text{jets}} \geq 7, N_{\text{b-tags}} = 0$ | | | | | | | |
| 200–300 | 7.44 \pm 2.01 | 8.20 \pm 1.16 | 1.77 \pm 0.87 | 12.1 \pm 1.9 | 29.5 \pm 3.2 | 29 | |
| 300–370 | 4.19 \pm 1.59 | 2.28 \pm 0.35 | 0.717 \pm 0.580 | 0.00729 \pm 0.00370 | 7.19 \pm 1.70 | 5 | |
| 370–450 | 1.40 \pm 0.88 | 1.72 \pm 0.29 | 0.200 \pm 0.124 | 0.362 \pm 0.184 | 3.68 \pm 0.97 | 1 | |
| 450–600 | 1.40 \pm 0.79 | 1.22 \pm 0.27 | 0.0115 \pm 0.0139 | 0.515 \pm 0.261 | 3.14 \pm 0.86 | 2 | |
| ≥ 600 | 0.931 \pm 0.786 | 0.695 \pm 0.161 | 0.0271 \pm 0.0397 | 0 \pm 0.00508 | 1.66 \pm 0.81 | 1 | |
| $2 \leq N_{\text{jets}} \leq 4, N_{\text{b-tags}} \geq 1$ | | | | | | | |
| 200–300 | 238 \pm 22 | 139 \pm 29 | 57.0 \pm 19.6 | 241 \pm 91 | 675 \pm 94 | 674 | |
| 300–370 | 53.9 \pm 7.9 | 30.3 \pm 6.3 | 19.1 \pm 7.6 | 14.4 \pm 6.6 | 118 \pm 14 | 114 | |
| 370–450 | 19.1 \pm 4.0 | 14.0 \pm 3.0 | 8.35 \pm 3.90 | 4.52 \pm 2.08 | 46.0 \pm 6.4 | 58 | |
| 450–600 | 13.0 \pm 3.4 | 7.45 \pm 1.64 | 7.80 \pm 4.08 | 1.86 \pm 0.85 | 30.1 \pm 5.5 | 35 | |
| ≥ 600 | 3.47 \pm 1.56 | 2.30 \pm 0.58 | 3.00 \pm 2.31 | 0.242 \pm 0.111 | 9.02 \pm 2.73 | 6 | |
| $5 \leq N_{\text{jets}} \leq 6, N_{\text{b-tags}} \geq 1$ | | | | | | | |
| 200–300 | 77.6 \pm 9.8 | 62.4 \pm 13.6 | 1.55 \pm 1.09 | 53.2 \pm 10.0 | 195 \pm 19 | 194 | |
| 300–370 | 17.2 \pm 3.9 | 16.7 \pm 3.7 | 1.26 \pm 0.77 | 7.57 \pm 2.33 | 42.7 \pm 5.9 | 48 | |
| 370–450 | 8.24 \pm 2.46 | 7.31 \pm 1.59 | 0.672 \pm 0.633 | 1.54 \pm 0.48 | 17.8 \pm 3.1 | 23 | |
| 450–600 | 2.06 \pm 1.11 | 4.25 \pm 0.95 | 0.0772 \pm 0.0616 | 0 \pm 0.00308 | 6.39 \pm 1.46 | 8 | |
| ≥ 600 | 2.06 \pm 1.15 | 1.27 \pm 0.29 | 0.0587 \pm 0.0452 | 1.41 \pm 0.44 | 4.81 \pm 1.22 | 3 | |
| $N_{\text{jets}} \geq 7, N_{\text{b-tags}} \geq 1$ | | | | | | | |
| 200–300 | 18.3 \pm 4.0 | 24.2 \pm 5.1 | 0.0767 \pm 0.0579 | 22.1 \pm 7.5 | 64.6 \pm 10.0 | 64 | |
| 300–370 | 5.89 \pm 2.02 | 7.14 \pm 1.65 | 0.697 \pm 0.567 | 1.48 \pm 1.02 | 15.2 \pm 2.9 | 8 | |
| 370–450 | 4.12 \pm 1.58 | 3.31 \pm 0.71 | 0.0600 \pm 0.0555 | 0.573 \pm 0.395 | 8.07 \pm 1.76 | 9 | |
| 450–600 | 2.95 \pm 1.36 | 2.04 \pm 0.47 | 0 \pm 0.00472 | 0.364 \pm 0.251 | 5.36 \pm 1.48 | 3 | |
| ≥ 600 | 1.18 \pm 0.84 | 0.581 \pm 0.223 | 0.0270 \pm 0.0283 | 0 \pm 0.00689 | 1.80 \pm 0.83 | 1 | |
| V-tag | | | | | | | |
| 200–300 | 172 \pm 17 | 174 \pm 35 | 39.2 \pm 8.1 | 180 \pm 51 | 565 \pm 63 | 564 | |
| 300–370 | 47.8 \pm 8.4 | 34.9 \pm 7.6 | 11.6 \pm 3.6 | 8.57 \pm 4.06 | 103 \pm 13 | 97 | |
| 370–450 | 19.8 \pm 4.9 | 13.0 \pm 2.9 | 9.80 \pm 3.38 | 3.60 \pm 1.71 | 46.2 \pm 7.2 | 52 | |
| 450–600 | 12.5 \pm 3.2 | 6.02 \pm 1.37 | 8.48 \pm 3.55 | 0.952 \pm 0.451 | 27.9 \pm 5.2 | 36 | |
| 600–750 | 7.28 \pm 2.91 | 1.38 \pm 0.34 | 2.88 \pm 1.72 | 0.334 \pm 0.158 | 11.9 \pm 3.4 | 4 | |
| ≥ 750 | 2.08 \pm 1.37 | 0.670 \pm 0.178 | 1.78 \pm 1.52 | 0 \pm 0.00473 | 4.54 \pm 2.01 | 2 | |
| H-tag | | | | | | | |
| 200–300 | 76.3 \pm 10.3 | 88.2 \pm 18.7 | 14.1 \pm 3.7 | 67.5 \pm 15.3 | 246 \pm 27 | 245 | |
| 300–370 | 24.1 \pm 5.4 | 24.2 \pm 5.1 | 5.73 \pm 2.20 | 6.75 \pm 2.94 | 60.7 \pm 8.3 | 60 | |
| 370–450 | 7.02 \pm 2.83 | 10.5 \pm 2.2 | 5.28 \pm 2.41 | 2.83 \pm 1.23 | 25.6 \pm 4.5 | 34 | |
| 450–600 | 9.03 \pm 2.98 | 4.62 \pm 1.05 | 4.02 \pm 2.15 | 0 \pm 0.00436 | 17.7 \pm 3.8 | 20 | |
| 600–750 | 3.01 \pm 1.76 | 1.02 \pm 0.28 | 2.56 \pm 1.34 | 0.706 \pm 0.308 | 7.30 \pm 2.28 | 2 | |
| ≥ 750 | 2.01 \pm 1.40 | 0.504 \pm 0.144 | 1.19 \pm 1.05 | 0 \pm 0.00436 | 3.72 \pm 1.66 | 2 | |

Table 3. The number of events predicted and observed for the signal regions and the low- p_T^{miss} regions used for the estimation of the γ +jets and QCD multijet backgrounds.

Open Access. This article is distributed under the terms of the Creative Commons Attribution License ([CC-BY 4.0](#)), which permits any use, distribution and reproduction in any medium, provided the original author(s) and source are credited.

References

- [1] F. Zwicky, *Die Rotverschiebung von extragalaktischen Nebeln* (in German), *Helv. Phys. Acta* **6** (1933) 110 [[INSPIRE](#)].
- [2] V.C. Rubin and W.K. Ford Jr., *Rotation of the Andromeda nebula from a spectroscopic survey of emission regions*, *Astrophys. J.* **159** (1970) 379 [[INSPIRE](#)].
- [3] R. Barbieri and G.F. Giudice, *Upper bounds on supersymmetric particle masses*, *Nucl. Phys. B* **306** (1988) 63 [[INSPIRE](#)].
- [4] S. Dimopoulos and G.F. Giudice, *Naturalness constraints in supersymmetric theories with nonuniversal soft terms*, *Phys. Lett. B* **357** (1995) 573 [[hep-ph/9507282](#)] [[INSPIRE](#)].
- [5] R. Barbieri and D. Pappadopulo, *S-particles at their naturalness limits*, *JHEP* **10** (2009) 061 [[arXiv:0906.4546](#)] [[INSPIRE](#)].
- [6] M. Papucci, J.T. Ruderman and A. Weiler, *Natural SUSY endures*, *JHEP* **09** (2012) 035 [[arXiv:1110.6926](#)] [[INSPIRE](#)].
- [7] P. Ramond, *Dual theory for free fermions*, *Phys. Rev. D* **3** (1971) 2415 [[INSPIRE](#)].
- [8] Y.A. Golfand and E.P. Likhtman, *Extension of the algebra of Poincaré group generators and violation of p invariance*, *JETP Lett.* **13** (1971) 323 [[INSPIRE](#)].
- [9] A. Neveu and J.H. Schwarz, *Factorizable dual model of pions*, *Nucl. Phys. B* **31** (1971) 86 [[INSPIRE](#)].
- [10] D.V. Volkov and V.P. Akulov, *Possible universal neutrino interaction*, *JETP Lett.* **16** (1972) 438 [[INSPIRE](#)].
- [11] J. Wess and B. Zumino, *A Lagrangian model invariant under supergauge transformations*, *Phys. Lett. B* **49** (1974) 52 [[INSPIRE](#)].
- [12] J. Wess and B. Zumino, *Supergauge transformations in four-dimensions*, *Nucl. Phys. B* **70** (1974) 39 [[INSPIRE](#)].
- [13] P. Fayet, *Supergauge invariant extension of the Higgs mechanism and a model for the electron and its neutrino*, *Nucl. Phys. B* **90** (1975) 104 [[INSPIRE](#)].
- [14] H.P. Nilles, *Supersymmetry, supergravity and particle physics*, *Phys. Rept.* **110** (1984) 1 [[INSPIRE](#)].
- [15] G.R. Farrar and P. Fayet, *Phenomenology of the production, decay, and detection of new hadronic states associated with supersymmetry*, *Phys. Lett. B* **76** (1978) 575 [[INSPIRE](#)].
- [16] D. Emmanuel-Costa, P. Fileviez Perez and R. Gonzalez Felipe, *Natural gauge and gravitational coupling unification and the superpartner masses*, *Phys. Lett. B* **648** (2007) 60 [[hep-ph/0610178](#)] [[INSPIRE](#)].
- [17] H. Baer et al., *Radiative natural SUSY with a 125 GeV Higgs boson*, *Phys. Rev. Lett.* **109** (2012) 161802 [[arXiv:1207.3343](#)] [[INSPIRE](#)].
- [18] P. Fayet, *Mixing between gravitational and weak interactions through the massive gravitino*, *Phys. Lett. B* **70** (1977) 461 [[INSPIRE](#)].

- [19] H. Baer, M. Brhlik, C.-H. Chen and X. Tata, *Signals for the minimal gauge mediated supersymmetry breaking model at the Fermilab Tevatron collider*, *Phys. Rev. D* **55** (1997) 4463 [[hep-ph/9610358](#)] [[INSPIRE](#)].
- [20] N. Arkani-Hamed et al., *MARMOSET: the path from LHC data to the new Standard Model via on-shell effective theories*, [hep-ph/0703088](#) [[INSPIRE](#)].
- [21] J. Alwall, P. Schuster and N. Toro, *Simplified models for a first characterization of new physics at the LHC*, *Phys. Rev. D* **79** (2009) 075020 [[arXiv:0810.3921](#)] [[INSPIRE](#)].
- [22] J. Alwall, M.-P. Le, M. Lisanti and J.G. Wacker, *Model-independent jets plus missing energy searches*, *Phys. Rev. D* **79** (2009) 015005 [[arXiv:0809.3264](#)] [[INSPIRE](#)].
- [23] LHC NEW PHYSICS WORKING GROUP collaboration, *Simplified models for LHC new physics searches*, *J. Phys. G* **39** (2012) 105005 [[arXiv:1105.2838](#)] [[INSPIRE](#)].
- [24] CMS collaboration, *Interpretation of searches for supersymmetry with simplified models*, *Phys. Rev. D* **88** (2013) 052017 [[arXiv:1301.2175](#)] [[INSPIRE](#)].
- [25] CMS collaboration, *Search for gauge-mediated supersymmetry in events with at least one photon and missing transverse momentum in pp collisions at $\sqrt{s} = 13$ TeV*, *Phys. Lett. B* **780** (2018) 118 [[arXiv:1711.08008](#)] [[INSPIRE](#)].
- [26] CMS collaboration, *Search for supersymmetry in events with at least one photon, missing transverse momentum, and large transverse event activity in proton-proton collisions at $\sqrt{s} = 13$ TeV*, *JHEP* **12** (2017) 142 [[arXiv:1707.06193](#)] [[INSPIRE](#)].
- [27] CMS collaboration, *Search for supersymmetry in events with a photon, jets, b-jets, and missing transverse momentum in proton-proton collisions at 13 TeV*, *Eur. Phys. J. C* **79** (2019) 444 [[arXiv:1901.06726](#)] [[INSPIRE](#)].
- [28] ATLAS collaboration, *Search for supersymmetry in a final state containing two photons and missing transverse momentum in $\sqrt{s} = 13$ TeV pp collisions at the LHC using the ATLAS detector*, *Eur. Phys. J. C* **76** (2016) 517 [[arXiv:1606.09150](#)] [[INSPIRE](#)].
- [29] ATLAS collaboration, *Search for photonic signatures of gauge-mediated supersymmetry in 13 TeV pp collisions with the ATLAS detector*, *Phys. Rev. D* **97** (2018) 092006 [[arXiv:1802.03158](#)] [[INSPIRE](#)].
- [30] ATLAS collaboration, *Search for new phenomena in final states with photons, jets and missing transverse momentum in pp collisions at $\sqrt{s} = 13$ TeV with the ATLAS detector*, *JHEP* **07** (2023) 021 [[arXiv:2206.06012](#)] [[INSPIRE](#)].
- [31] CMS collaboration, *HEPData record for this analysis*, (2023) [[DOI:10.17182/hepdata.140958](#)].
- [32] CMS collaboration, *The CMS experiment at the CERN LHC*, 2008 *JINST* **3** S08004 [[INSPIRE](#)].
- [33] CMS collaboration, *The CMS trigger system*, 2017 *JINST* **12** P01020 [[arXiv:1609.02366](#)] [[INSPIRE](#)].
- [34] CMS collaboration, *Particle-flow reconstruction and global event description with the CMS detector*, 2017 *JINST* **12** P10003 [[arXiv:1706.04965](#)] [[INSPIRE](#)].
- [35] D. Contardo et al., *Technical proposal for the phase-II upgrade of the CMS detector*, CERN-LHCC-2015-010, CERN, Geneva, Switzerland (2015) [[DOI:10.17181/CERN.VU8I.D59J](#)].
- [36] M. Cacciari, G.P. Salam and G. Soyez, *The anti- k_t jet clustering algorithm*, *JHEP* **04** (2008) 063 [[arXiv:0802.1189](#)] [[INSPIRE](#)].

- [37] M. Cacciari, G.P. Salam and G. Soyez, *FastJet user manual*, *Eur. Phys. J. C* **72** (2012) 1896 [[arXiv:1111.6097](#)] [[INSPIRE](#)].
- [38] M. Cacciari and G.P. Salam, *Pileup subtraction using jet areas*, *Phys. Lett. B* **659** (2008) 119 [[arXiv:0707.1378](#)] [[INSPIRE](#)].
- [39] CMS collaboration, *Pileup mitigation at CMS in 13 TeV data*, *2020 JINST* **15** P09018 [[arXiv:2003.00503](#)] [[INSPIRE](#)].
- [40] CMS collaboration, *Jet energy scale and resolution in the CMS experiment in pp collisions at 8 TeV*, *2017 JINST* **12** P02014 [[arXiv:1607.03663](#)] [[INSPIRE](#)].
- [41] CMS collaboration, *Jet algorithms performance in 13 TeV data*, CMS-PAS-JME-16-003, CERN, Geneva, Switzerland (2017).
- [42] A.J. Larkoski, S. Marzani, G. Soyez and J. Thaler, *Soft drop*, *JHEP* **05** (2014) 146 [[arXiv:1402.2657](#)] [[INSPIRE](#)].
- [43] CMS collaboration, *Identification of heavy-flavour jets with the CMS detector in pp collisions at 13 TeV*, *2018 JINST* **13** P05011 [[arXiv:1712.07158](#)] [[INSPIRE](#)].
- [44] CMS collaboration, *Performance of missing transverse momentum reconstruction in proton-proton collisions at $\sqrt{s} = 13$ TeV using the CMS detector*, *2019 JINST* **14** P07004 [[arXiv:1903.06078](#)] [[INSPIRE](#)].
- [45] CMS collaboration, *Electron and photon reconstruction and identification with the CMS experiment at the CERN LHC*, *2021 JINST* **16** P05014 [[arXiv:2012.06888](#)] [[INSPIRE](#)].
- [46] CMS collaboration, *Performance of the CMS muon detector and muon reconstruction with proton-proton collisions at $\sqrt{s} = 13$ TeV*, *2018 JINST* **13** P06015 [[arXiv:1804.04528](#)] [[INSPIRE](#)].
- [47] J. Alwall et al., *The automated computation of tree-level and next-to-leading order differential cross sections, and their matching to parton shower simulations*, *JHEP* **07** (2014) 079 [[arXiv:1405.0301](#)] [[INSPIRE](#)].
- [48] J. Alwall et al., *Comparative study of various algorithms for the merging of parton showers and matrix elements in hadronic collisions*, *Eur. Phys. J. C* **53** (2008) 473 [[arXiv:0706.2569](#)] [[INSPIRE](#)].
- [49] T. Sjöstrand et al., *An introduction to PYTHIA 8.2*, *Comput. Phys. Commun.* **191** (2015) 159 [[arXiv:1410.3012](#)] [[INSPIRE](#)].
- [50] NNPDF collaboration, *Parton distributions for the LHC run II*, *JHEP* **04** (2015) 040 [[arXiv:1410.8849](#)] [[INSPIRE](#)].
- [51] NNPDF collaboration, *Parton distributions from high-precision collider data*, *Eur. Phys. J. C* **77** (2017) 663 [[arXiv:1706.00428](#)] [[INSPIRE](#)].
- [52] CMS collaboration, *Event generator tunes obtained from underlying event and multiparton scattering measurements*, *Eur. Phys. J. C* **76** (2016) 155 [[arXiv:1512.00815](#)] [[INSPIRE](#)].
- [53] CMS collaboration, *Extraction and validation of a new set of CMS PYTHIA8 tunes from underlying-event measurements*, *Eur. Phys. J. C* **80** (2020) 4 [[arXiv:1903.12179](#)] [[INSPIRE](#)].
- [54] R. Frederix and S. Frixione, *Merging meets matching in MC@NLO*, *JHEP* **12** (2012) 061 [[arXiv:1209.6215](#)] [[INSPIRE](#)].

- [55] A. Kulesza and L. Motyka, *Soft gluon resummation for the production of gluino-gluino and squark-antisquark pairs at the LHC*, *Phys. Rev. D* **80** (2009) 095004 [[arXiv:0905.4749](#)] [[INSPIRE](#)].
- [56] W. Beenakker et al., *Soft-gluon resummation for squark and gluino hadroproduction*, *JHEP* **12** (2009) 041 [[arXiv:0909.4418](#)] [[INSPIRE](#)].
- [57] W. Beenakker et al., *NNLL resummation for squark-antisquark pair production at the LHC*, *JHEP* **01** (2012) 076 [[arXiv:1110.2446](#)] [[INSPIRE](#)].
- [58] W. Beenakker et al., *Towards NNLL resummation: hard matching coefficients for squark and gluino hadroproduction*, *JHEP* **10** (2013) 120 [[arXiv:1304.6354](#)] [[INSPIRE](#)].
- [59] W. Beenakker et al., *NNLL resummation for squark and gluino production at the LHC*, *JHEP* **12** (2014) 023 [[arXiv:1404.3134](#)] [[INSPIRE](#)].
- [60] W. Beenakker et al., *NNLL resummation for stop pair-production at the LHC*, *JHEP* **05** (2016) 153 [[arXiv:1601.02954](#)] [[INSPIRE](#)].
- [61] W. Beenakker et al., *NNLL-fast: predictions for coloured supersymmetric particle production at the LHC with threshold and Coulomb resummation*, *JHEP* **12** (2016) 133 [[arXiv:1607.07741](#)] [[INSPIRE](#)].
- [62] GEANT4 collaboration, *GEANT4 — a simulation toolkit*, *Nucl. Instrum. Meth. A* **506** (2003) 250 [[INSPIRE](#)].
- [63] CMS collaboration, *The fast simulation of the CMS detector at LHC*, *J. Phys. Conf. Ser.* **331** (2011) 032049 [[INSPIRE](#)].
- [64] A. Giiammanco, *The fast simulation of the CMS experiment*, *J. Phys. Conf. Ser.* **513** (2014) 022012 [[INSPIRE](#)].
- [65] CMS collaboration, *Measurement of the inclusive and differential $t\bar{t}\gamma$ cross sections in the single-lepton channel and EFT interpretation at $\sqrt{s} = 13$ TeV*, *JHEP* **12** (2021) 180 [[arXiv:2107.01508](#)] [[INSPIRE](#)].
- [66] M. Cacciari et al., *The $t\bar{t}$ cross-section at 1.8 TeV and 1.96 TeV: a study of the systematics due to parton densities and scale dependence*, *JHEP* **04** (2004) 068 [[hep-ph/0303085](#)] [[INSPIRE](#)].
- [67] S. Catani, D. de Florian, M. Grazzini and P. Nason, *Soft gluon resummation for Higgs boson production at hadron colliders*, *JHEP* **07** (2003) 028 [[hep-ph/0306211](#)] [[INSPIRE](#)].
- [68] CMS collaboration, *Measurements of inclusive W and Z cross sections in pp collisions at $\sqrt{s} = 7$ TeV*, *JHEP* **01** (2011) 080 [[arXiv:1012.2466](#)] [[INSPIRE](#)].
- [69] A. Denner, S. Dittmaier, M. Hecht and C. Pasold, *NLO QCD and electroweak corrections to $Z + \gamma$ production with leptonic Z -boson decays*, *JHEP* **02** (2016) 057 [[arXiv:1510.08742](#)] [[INSPIRE](#)].
- [70] CMS collaboration, *Precision luminosity measurement in proton-proton collisions at $\sqrt{s} = 13$ TeV in 2015 and 2016 at CMS*, *Eur. Phys. J. C* **81** (2021) 800 [[arXiv:2104.01927](#)] [[INSPIRE](#)].
- [71] CMS collaboration, *CMS luminosity measurement for the 2017 data-taking period at $\sqrt{s} = 13$ TeV*, **CMS-PAS-LUM-17-004**, CERN, Geneva, Switzerland (2018).
- [72] CMS collaboration, *CMS luminosity measurement for the 2018 data-taking period at $\sqrt{s} = 13$ TeV*, **CMS-PAS-LUM-18-002**, CERN, Geneva, Switzerland (2019).

- [73] CMS collaboration, *Search for supersymmetry in proton-proton collisions at 13 TeV in final states with jets and missing transverse momentum*, *JHEP* **10** (2019) 244 [[arXiv:1908.04722](#)] [[INSPIRE](#)].
- [74] T. Junk, *Confidence level computation for combining searches with small statistics*, *Nucl. Instrum. Meth. A* **434** (1999) 435 [[hep-ex/9902006](#)] [[INSPIRE](#)].
- [75] A.L. Read, *Presentation of search results: the CL_s technique*, *J. Phys. G* **28** (2002) 2693 [[INSPIRE](#)].
- [76] G. Cowan, K. Cranmer, E. Gross and O. Vitells, *Asymptotic formulae for likelihood-based tests of new physics*, *Eur. Phys. J. C* **71** (2011) 1554 [*Erratum ibid.* **73** (2013) 2501] [[arXiv:1007.1727](#)] [[INSPIRE](#)].

The CMS collaboration

Yerevan Physics Institute, Yerevan, Armenia

A. Hayrapetyan, A. Tumasyan¹

Institut für Hochenergiephysik, Vienna, Austria

W. Adam¹, J.W. Andrejkovic, T. Bergauer¹, S. Chatterjee¹, K. Damanakis¹, M. Dragicevic¹, A. Escalante Del Valle¹, P.S. Hussain¹, M. Jeitler^{1,2}, N. Krammer¹, D. Liko¹, I. Mikulec¹, J. Schieck^{1,2}, R. Schöfbeck¹, D. Schwarz¹, M. Sonawane¹, S. Templ¹, W. Waltenberger¹, C.-E. Wulz^{1,2}

Universiteit Antwerpen, Antwerpen, Belgium

M.R. Darwish³, T. Janssen¹, P. Van Mechelen¹

Vrije Universiteit Brussel, Brussel, Belgium

E.S. Bols¹, J. D'Hondt¹, S. Dansana¹, A. De Moor¹, M. Delcourt¹, H. El Faham¹, S. Lowette¹, I. Makarenko¹, A. Morton¹, D. Müller¹, A.R. Sahasransu¹, S. Tavernier¹, M. Tytgat^{1,4}, S. Van Putte¹, D. Vannerom¹

Université Libre de Bruxelles, Bruxelles, Belgium

B. Clerbaux¹, G. De Lentdecker¹, L. Favart¹, D. Hohov¹, J. Jaramillo¹, A. Khalilzadeh, K. Lee¹, M. Mahdavikhorrami¹, A. Malara¹, S. Paredes¹, L. Pétré¹, N. Postiau, L. Thomas¹, M. Vanden Bemden¹, C. Vander Velde¹, P. Vanlaer¹

Ghent University, Ghent, Belgium

M. De Coen¹, D. Dobur¹, J. Knolle¹, L. Lambrecht¹, G. Mestdach, C. Rendón, A. Samalan, K. Skovpen¹, N. Van Den Bossche¹, L. Wezenbeek¹

Université Catholique de Louvain, Louvain-la-Neuve, Belgium

A. Benecke¹, G. Bruno¹, C. Caputo¹, C. Delaere¹, I.S. Donertas¹, A. Giannanco¹, K. Jaffel¹, Sa. Jain¹, V. Lemaitre, J. Lidrych¹, P. Mastrapasqua¹, K. Mondal¹, T.T. Tran¹, S. Wertz¹

Centro Brasileiro de Pesquisas Fisicas, Rio de Janeiro, Brazil

G.A. Alves¹, E. Coelho¹, C. Hensel¹, T. Menezes De Oliveira, A. Moraes¹, P. Rebello Teles¹, M. Soeiro

Universidade do Estado do Rio de Janeiro, Rio de Janeiro, Brazil

W.L. Aldá Júnior¹, M. Alves Gallo Pereira¹, M. Barroso Ferreira Filho¹, H. Brandao Malbouisson¹, W. Carvalho¹, J. Chinellato⁵, E.M. Da Costa¹, G.G. Da Silveira^{1,6}, D. De Jesus Damiao¹, S. Fonseca De Souza¹, J. Martins^{1,7}, C. Mora Herrera¹, K. Mota Amarilo¹, L. Mundim¹, H. Nogima¹, A. Santoro¹, S.M. Silva Do Amaral¹, A. Sznajder¹, M. Thiel¹, A. Vilela Pereira¹

**Universidade Estadual Paulista, Universidade Federal do ABC, São Paulo,
Brazil**

C.A. Bernardes⁶, L. Calligaris¹⁰, T.R. Fernandez Perez Tomei¹⁰, E.M. Gregores¹⁰,
P.G. Mercadante¹⁰, S.F. Novaes¹⁰, B. Orzari¹⁰, Sandra S. Padula¹⁰

**Institute for Nuclear Research and Nuclear Energy, Bulgarian Academy of
Sciences, Sofia, Bulgaria**

A. Aleksandrov¹⁰, G. Antchev¹⁰, R. Hadjiiska¹⁰, P. Iaydjiev¹⁰, M. Misheva¹⁰, M. Shopova¹⁰,
G. Sultanov¹⁰

University of Sofia, Sofia, Bulgaria

A. Dimitrov¹⁰, T. Ivanov¹⁰, L. Litov¹⁰, B. Pavlov¹⁰, P. Petkov¹⁰, A. Petrov¹⁰, E. Shumka¹⁰

**Instituto De Alta Investigación, Universidad de Tarapacá, Casilla 7 D, Arica,
Chile**

S. Keshri¹⁰, S. Thakur¹⁰

Beihang University, Beijing, China

T. Cheng¹⁰, Q. Guo, T. Javaid¹⁰, M. Mittal¹⁰, L. Yuan¹⁰

Department of Physics, Tsinghua University, Beijing, China

G. Bauer⁸, Z. Hu¹⁰, K. Yi^{10,8,9}

Institute of High Energy Physics, Beijing, China

G.M. Chen¹⁰, H.S. Chen¹⁰, M. Chen¹⁰, F. Iemmi¹⁰, C.H. Jiang, A. Kapoor¹⁰, H. Liao¹⁰,
Z.-A. Liu¹¹, F. Monti¹⁰, R. Sharma¹⁰, J.N. Song¹¹, J. Tao¹⁰, J. Wang¹⁰, H. Zhang¹⁰

**State Key Laboratory of Nuclear Physics and Technology, Peking University,
Beijing, China**

A. Agapitos¹⁰, Y. Ban¹⁰, A. Levin¹⁰, C. Li¹⁰, Q. Li¹⁰, X. Lyu, Y. Mao, S.J. Qian¹⁰, X. Sun¹⁰,
D. Wang¹⁰, H. Yang, C. Zhou¹⁰

Sun Yat-Sen University, Guangzhou, China

Z. You¹⁰

University of Science and Technology of China, Hefei, China

N. Lu¹⁰

**Institute of Modern Physics and Key Laboratory of Nuclear Physics and
Ion-beam Application (MOE) — Fudan University, Shanghai, China**

X. Gao¹², D. Leggat, H. Okawa¹⁰, Y. Zhang¹⁰

Zhejiang University, Hangzhou, Zhejiang, China

Z. Lin¹⁰, C. Lu¹⁰, M. Xiao¹⁰

Universidad de Los Andes, Bogota, Colombia

C. Avila¹⁰, D.A. Barbosa Trujillo, A. Cabrera¹⁰, C. Florez¹⁰, J. Fraga¹⁰, J.A. Reyes Vega

Universidad de Antioquia, Medellin, ColombiaJ. Mejia Guisao , F. Ramirez , M. Rodriguez , J.D. Ruiz Alvarez **University of Split, Faculty of Electrical Engineering, Mechanical Engineering and Naval Architecture, Split, Croatia**D. Giljanovic , N. Godinovic , D. Lelas , A. Sculac **University of Split, Faculty of Science, Split, Croatia**M. Kovac , T. Sculac **Institute Rudjer Boskovic, Zagreb, Croatia**P. Bargassa , V. Brigljevic , B.K. Chitroda , D. Ferencek , S. Mishra , A. Starodumov ¹³, T. Susa **University of Cyprus, Nicosia, Cyprus**A. Attikis , K. Christoforou , S. Konstantinou , J. Mousa , C. Nicolaou, F. Ptochos , P.A. Razis , H. Rykaczewski, H. Saka , A. Stepennov **Charles University, Prague, Czech Republic**M. Finger , M. Finger Jr. , A. Kveton **Escuela Politecnica Nacional, Quito, Ecuador**E. Ayala **Universidad San Francisco de Quito, Quito, Ecuador**E. Carrera Jarrin **Academy of Scientific Research and Technology of the Arab Republic of Egypt, Egyptian Network of High Energy Physics, Cairo, Egypt**H. Abdalla ¹⁴, Y. Assran^{15,16}**Center for High Energy Physics (CHEP-FU), Fayoum University, El-Fayoum, Egypt**M. Abdullah Al-Mashad , M.A. Mahmoud **National Institute of Chemical Physics and Biophysics, Tallinn, Estonia**R.K. Dewanjee ¹⁷, K. Ehataht , M. Kadastik, T. Lange , S. Nandan , C. Nielsen , J. Pata , M. Raidal , L. Tani , C. Veelken **Department of Physics, University of Helsinki, Helsinki, Finland**H. Kirschenmann , K. Osterberg , M. Voutilainen **Helsinki Institute of Physics, Helsinki, Finland**S. Bharthuar , E. Brücken , F. Garcia , J. Havukainen , K.T.S. Kallonen , M.S. Kim , R. Kinnunen, T. Lampén , K. Lassila-Perini , S. Lehti , T. Lindén , M. Lotti,

L. Martikainen , M. Myllymäki , M.m. Rantanen , H. Siikonen , E. Tuominen ,
J. Tuominiemi

Lappeenranta-Lahti University of Technology, Lappeenranta, Finland
P. Luukka , H. Petrow , T. Tuuva[†]

IRFU, CEA, Université Paris-Saclay, Gif-sur-Yvette, France

M. Besancon , F. Couderc , M. Dejardin , D. Denegri, J.L. Faure, F. Ferri , S. Ganjour ,
P. Gras , G. Hamel de Monchenault , V. Lohezic , J. Malcles , J. Rander, A. Rosowsky ,
M.Ö. Sahin , A. Savoy-Navarro ¹⁸, P. Simkina , M. Titov

Laboratoire Leprince-Ringuet, CNRS/IN2P3, Ecole Polytechnique, Institut Polytechnique de Paris, Palaiseau, France

C. Baldenegro Barrera , F. Beaudette , A. Buchot Perraguin , P. Busson , A. Cappati ,
C. Charlot , F. Damas , O. Davignon , G. Falmagne , B.A. Fontana Santos Alves ,
S. Ghosh , A. Gilbert , R. Granier de Cassagnac , A. Hakimi , B. Harikrishnan ,
L. Kalipoliti , G. Liu , J. Motta , M. Nguyen , C. Ochando , L. Portales , R. Salerno ,
U. Sarkar , J.B. Sauvan , Y. Sirois , A. Tarabini , E. Vernazza , A. Zabi , A. Zghiche

Université de Strasbourg, CNRS, IPHC UMR 7178, Strasbourg, France

J.-L. Agram ¹⁹, J. Andrea , D. Apparu , D. Bloch , J.-M. Brom , E.C. Chabert ,
C. Collard , S. Falke , U. Goerlach , C. Grimault, R. Haeberle, A.-C. Le Bihan ,
M.A. Sessini , P. Van Hove

Institut de Physique des 2 Infinis de Lyon (IP2I), Villeurbanne, France

S. Beauceron , B. Blancon , G. Boudoul , N. Chanon , J. Choi , D. Contardo ,
P. Depasse , C. Dozen ²⁰, H. El Mamouni, J. Fay , S. Gascon , M. Gouzevitch ,
C. Greenberg, G. Grenier , B. Ille , I.B. Laktineh, M. Lethuillier , L. Mirabito, S. Perries,
M. Vander Donckt , P. Verdier , J. Xiao

Georgian Technical University, Tbilisi, Georgia

I. Lomidze , T. Toriashvili ²¹, Z. Tsamalaidze ¹³

RWTH Aachen University, I. Physikalisches Institut, Aachen, Germany

V. Botta , L. Feld , K. Klein , M. Lipinski , D. Meuser , A. Pauls , N. Röwert ,
M. Teroerde

RWTH Aachen University, III. Physikalisches Institut A, Aachen, Germany

S. Diekmann , A. Dodonova , N. Eich , D. Eliseev , F. Engelke , M. Erdmann ,
P. Fackeldey , B. Fischer , T. Hebbeker , K. Hoepfner , F. Ivone , A. Jung , M.y. Lee ,
L. Mastrolorenzo, M. Merschmeyer , A. Meyer , S. Mukherjee , D. Noll , A. Novak ,
F. Nowotny, A. Pozdnyakov , Y. Rath, W. Redjeb , F. Rehm, H. Reithler , V. Sarkisovi ,
A. Schmidt , S.C. Schuler, A. Sharma , A. Stein , F. Torres Da Silva De Araujo ²²,
L. Vigilante, S. Wiedenbeck , S. Zaleski

RWTH Aachen University, III. Physikalisches Institut B, Aachen, Germany

C. Dziwok , G. Flügge , W. Haj Ahmad ²³, T. Kress , A. Nowack , O. Pooth ,
A. Stahl , T. Ziemons , A. Zottz 

Deutsches Elektronen-Synchrotron, Hamburg, Germany

H. Aarup Petersen , M. Aldaya Martin , J. Alimena , S. Amoroso, Y. An , S. Baxter ,
M. Bayatmakou , H. Becerril Gonzalez , O. Behnke , A. Belvedere , S. Bhattacharya ,
F. Blekman ²⁴, K. Borras ²⁵, D. Brunner , A. Campbell , A. Cardini , C. Cheng,
F. Colombina , S. Consuegra Rodríguez , G. Correia Silva , M. De Silva , G. Eckerlin,
D. Eckstein , L.I. Estevez Banos , O. Filatov , E. Gallo ²⁴, A. Geiser , A. Giraldi ,
G. Greau, V. Guglielmi , M. Guthoff , A. Hinzmamn , A. Jafari ²⁶, L. Jeppe ,
N.Z. Jomhari , B. Kaech , M. Kasemann , H. Kaveh , C. Kleinwort , R. Kogler ,
M. Komm , D. Krücker , W. Lange, D. Leyva Pernia , K. Lipka ²⁷, W. Lohmann ²⁸,
R. Mankel , I.-A. Melzer-Pellmann , M. Mendizabal Morentin , J. Metwally, A.B. Meyer ,
G. Milella , A. Mussgiller , A. Nürnberg , Y. Otariid, D. Pérez Adán , E. Ranken ,
A. Raspereza , B. Ribeiro Lopes , J. Rübenach, A. Saggio , M. Scham ^{29,25}, V. Scheurer,
S. Schnake , P. Schütze , C. Schwanenberger ²⁴, M. Shchedrolosiev , R.E. Sosa Ricardo ,
L.P. Sreelatha Pramod , D. Stafford, F. Vazzoler , A. Ventura Barroso , R. Walsh ,
Q. Wang , Y. Wen , K. Wichmann, L. Wiens ²⁵, C. Wissing , S. Wuchterl , Y. Yang ,
A. Zimermann Castro Santos

University of Hamburg, Hamburg, Germany

A. Albrecht , S. Albrecht , M. Antonello , S. Bein , L. Benato , M. Bonanomi ,
P. Connor , M. Eich, K. El Morabit , Y. Fischer , A. Fröhlich, C. Garbers , E. Garutti ,
A. Grohsjean , M. Hajheidari, J. Haller , H.R. Jabusch , G. Kasieczka , P. Keicher,
R. Klanner , W. Korcari , T. Kramer , V. Kutzner , F. Labe , J. Lange , A. Lobanov ,
C. Matthies , A. Mehta , L. Moureaux , M. Mrowietz, A. Nigamova , Y. Nissan,
A. Paasch , K.J. Pena Rodriguez , T. Quadfasel , B. Raciti , M. Rieger , D. Savoiu ,
J. Schindler , P. Schleper , M. Schröder , J. Schwandt , M. Sommerhalder , H. Stadie ,
G. Steinbrück , A. Tews, M. Wolf

Karlsruher Institut fuer Technologie, Karlsruhe, Germany

S. Brommer , M. Burkart, E. Butz , T. Chwalek , A. Dierlamm , A. Droll,
N. Faltermann , M. Giffels , A. Gottmann , F. Hartmann ³⁰, M. Horzela , U. Husemann ,
M. Klute , R. Koppenhöfer , M. Link, A. Lintuluoto , S. Maier , S. Mitra , M. Mormile ,
Th. Müller , M. Neukum, M. Oh , G. Quast , K. Rabbertz , I. Shvetsov , H.J. Simonis ,
N. Trevisani , R. Ulrich , J. van der Linden , R.F. Von Cube , M. Wassmer ,
S. Wieland , F. Wittig, R. Wolf , S. Wunsch, X. Zuo

Institute of Nuclear and Particle Physics (INPP), NCSR Demokritos, Aghia Paraskevi, Greece

G. Anagnostou, P. Assiouras , G. Daskalakis , A. Kyriakis, A. Papadopoulos ³⁰, A. Stakia 

National and Kapodistrian University of Athens, Athens, Greece

D. Karasavvas, P. Kontaxakis , G. Melachroinos, A. Panagiotou, I. Papavergou ,
I. Paraskevas , N. Saoulidou , K. Theofilatos , E. Tziaferi , K. Vellidis , I. Zisopoulos

National Technical University of Athens, Athens, Greece

G. Bakas , T. Chatzistavrou, G. Karapostoli , K. Kousouris , I. Papakrivopoulos ,
E. Siamarkou, G. Tsipolitis, A. Zacharopoulou

University of Ioánnina, Ioánnina, Greece

K. Adamidis, I. Bestintzanos, I. Evangelou , C. Foudas, P. Gianneios , C. Kamtsikis,
P. Katsoulis, P. Kokkas , P.G. Kosmoglou Kioseoglou , N. Manthos , I. Papadopoulos ,
J. Strologas

MTA-ELTE Lendület CMS Particle and Nuclear Physics Group, Eötvös Loránd University, Budapest, Hungary

M. Csanad , K. Farkas , M.M.A. Gadallah ³¹, . Kadlecseik , P. Major , K. Mandal ,
G. Pasztor , A.J. Radl ³², G.I. Veres

Wigner Research Centre for Physics, Budapest, Hungary

M. Bartok ³³, C. Hajdu , D. Horvath ^{34,35}, F. Sikler , V. Veszpremi

Institute of Nuclear Research ATOMKI, Debrecen, Hungary

G. Bencze, S. Czellar, J. Karancsi ³³, J. Molnar, Z. Szillasi

Institute of Physics, University of Debrecen, Debrecen, Hungary

P. Raics, B. Ujvari ³⁶, G. Zilizi

Karoly Robert Campus, MATE Institute of Technology, Gyongyos, Hungary

T. Csorgo ³², F. Nemes ³², T. Novak

Panjab University, Chandigarh, India

J. Babbar , S. Bansal , S.B. Beri, V. Bhatnagar , G. Chaudhary , S. Chauhan ,
N. Dhingra ³⁷, R. Gupta, A. Kaur , A. Kaur , H. Kaur , M. Kaur , S. Kumar ,
P. Kumari , M. Meena , K. Sandeep , T. Sheokand, J.B. Singh ³⁸, A. Singla

University of Delhi, Delhi, India

A. Ahmed , A. Bhardwaj , A. Chhetri , B.C. Choudhary , A. Kumar , M. Naimuddin ,
K. Ranjan , S. Saumya

Saha Institute of Nuclear Physics, HBNI, Kolkata, India

S. Baradia , S. Barman ³⁹, S. Bhattacharya , D. Bhowmik, S. Dutta , S. Dutta,
B. Gomber ⁴⁰, P. Palit , G. Saha , B. Sahu ⁴⁰, S. Sarkar

Indian Institute of Technology Madras, Madras, India

P.K. Behera , S.C. Behera , S. Chatterjee , P. Jana , P. Kalbhor , J.R. Komaragiri ⁴¹,
D. Kumar ⁴¹, M. Mohammad Mobassir Ameen , L. Panwar ⁴¹, R. Pradhan ,
P.R. Pujahari , N.R. Saha , A. Sharma , A.K. Sikdar , S. Verma

Tata Institute of Fundamental Research-A, Mumbai, IndiaT. Aziz, I. Das^{id}, S. Dugad, M. Kumar^{id}, G.B. Mohanty^{id}, P. Suryadevara**Tata Institute of Fundamental Research-B, Mumbai, India**A. Bala^{id}, S. Banerjee^{id}, R.M. Chatterjee, M. Guchait^{id}, S. Karmakar^{id}, S. Kumar^{id},
G. Majumder^{id}, K. Mazumdar^{id}, S. Mukherjee^{id}, A. Thachayath^{id}**National Institute of Science Education and Research, An OCC of Homi Bhabha National Institute, Bhubaneswar, Odisha, India**S. Bahinipati^{id}⁴², A.K. Das, C. Kar^{id}, D. Maity^{id}⁴³, P. Mal^{id}, T. Mishra^{id},
V.K. Muraleedharan Nair Bindhu^{id}⁴³, K. Naskar^{id}⁴³, A. Nayak^{id}⁴³, P. Sadangi, P. Saha^{id},
S.K. Swain^{id}, S. Varghese^{id}⁴³, D. Vats^{id}⁴³**Indian Institute of Science Education and Research (IISER), Pune, India**A. Alpana^{id}, S. Dube^{id}, B. Kansal^{id}, A. Laha^{id}, A. Rane^{id}, A. Rastogi^{id}, S. Sharma^{id}**Isfahan University of Technology, Isfahan, Iran**H. Bakhshiansohi^{id}⁴⁴, E. Khazaie^{id}⁴⁵, M. Zeinali^{id}⁴⁶**Institute for Research in Fundamental Sciences (IPM), Tehran, Iran**S. Chenarani^{id}⁴⁷, S.M. Etesami^{id}, M. Khakzad^{id}, M. Mohammadi Najafabadi^{id}**University College Dublin, Dublin, Ireland**M. Grunewald^{id}**INFN Sezione di Bari^a, Università di Bari^b, Politecnico di Bari^c, Bari, Italy**M. Abbrescia^{id}^{a,b}, R. Aly^{id}^{a,c,48}, A. Colaleo^{id}^a, D. Creanza^{id}^{a,c}, B. D' Anzi^{id}^{a,b},
N. De Filippis^{id}^{a,c}, M. De Palma^{id}^{a,b}, A. Di Florio^{id}^{a,c}, W. Elmetenawee^{id}^{a,b}, L. Fiore^{id}^a,
G. Iaselli^{id}^{a,c}, G. Maggi^{id}^{a,c}, M. Maggi^{id}^a, I. Margjeka^{id}^{a,b}, V. Mastrapasqua^{id}^{a,b}, S. My^{id}^{a,b},
S. Nuzzo^{id}^{a,b}, A. Pellecchia^{id}^{a,b}, A. Pompili^{id}^{a,b}, G. Pugliese^{id}^{a,c}, R. Radogna^{id}^a,
G. Ramirez-Sanchez^{id}^{a,c}, D. Ramos^{id}^a, A. Ranieri^{id}^a, L. Silvestris^{id}^a, F.M. Simone^{id}^{a,b},
Ü. Sözbilir^{id}^a, A. Stamerra^{id}^a, R. Venditti^{id}^a, P. Verwilligen^{id}^a, A. Zaza^{id}^{a,b}**INFN Sezione di Bologna^a, Università di Bologna^b, Bologna, Italy**G. Abbiendi^{id}^a, C. Battilana^{id}^{a,b}, D. Bonacorsi^{id}^{a,b}, L. Borgonovi^{id}^a, R. Campanini^{id}^{a,b},
P. Capiluppi^{id}^{a,b}, A. Castro^{id}^{a,b}, M. Cuffiani^{id}^{a,b}, G.M. Dallavalle^{id}^a, T. Diotalevi^{id}^{a,b},
F. Fabbri^{id}^a, A. Fanfani^{id}^{a,b}, D. Fasanella^{id}^{a,b}, P. Giacomelli^{id}^a, L. Giommi^{id}^{a,b}, C. Grandi^{id}^a,
L. Guiducci^{id}^{a,b}, S. Lo Meo^{id}^{a,49}, L. Lunerti^{id}^{a,b}, S. Marcellini^{id}^a, G. Masetti^{id}^a,
F.L. Navarrone^{id}^{a,b}, A. Perrotta^{id}^a, F. Primavera^{id}^{a,b}, A.M. Rossi^{id}^{a,b}, T. Rovelli^{id}^{a,b},
G.P. Siroli^{id}^{a,b}**INFN Sezione di Catania^a, Università di Catania^b, Catania, Italy**S. Costa^{id}^{a,b,50}, A. Di Mattia^{id}^a, R. Potenza^{a,b}, A. Tricomi^{id}^{a,b,50}, C. Tuve^{id}^{a,b}

INFN Sezione di Firenze^a, Università di Firenze^b, Firenze, Italy

G. Barbagli ^a, G. Bardelli ^{a,b}, B. Camaiani ^{a,b}, A. Cassese ^a, R. Ceccarelli ^a, V. Ciulli ^{a,b}, C. Civinini ^a, R. D'Alessandro ^{a,b}, E. Focardi ^{a,b}, G. Latino ^{a,b}, P. Lenzi ^{a,b}, M. Lizzo ^{a,b}, M. Meschini ^a, S. Paoletti ^a, A. Papanastassiou ^{a,b}, G. Sguazzoni ^a, L. Viliani ^a

INFN Laboratori Nazionali di Frascati, Frascati, Italy

L. Benussi , S. Bianco , S. Meola ⁵¹, D. Piccolo

INFN Sezione di Genova^a, Università di Genova^b, Genova, Italy

P. Chatagnon ^a, F. Ferro ^a, E. Robutti ^a, S. Tosi ^{a,b}

INFN Sezione di Milano-Bicocca^a, Università di Milano-Bicocca^b, Milano, Italy

A. Benaglia ^a, G. Boldrini ^a, F. Brivio ^a, F. Cetorelli ^a, F. De Guio ^{a,b}, M.E. Dinardo ^{a,b}, P. Dini ^a, S. Gennai ^a, A. Ghezzi ^{a,b}, P. Govoni ^{a,b}, L. Guzzi ^a, M.T. Lucchini ^{a,b}, M. Malberti ^a, S. Malvezzi ^a, A. Massironi ^a, D. Menasce ^a, L. Moroni ^a, M. Paganoni ^{a,b}, D. Pedrini ^a, B.S. Pinolini ^a, S. Ragazzi ^{a,b}, N. Redaelli ^a, T. Tabarelli de Fatis ^{a,b}, D. Zuolo

INFN Sezione di Napoli^a, Università di Napoli ‘Federico II’^b, Napoli, Italy; Università della Basilicata^c, Potenza, Italy; Università G. Marconi^d, Roma, Italy

S. Buontempo ^a, A. Cagnotta ^{a,b}, F. Carnevali ^{a,b}, N. Cavallo ^{a,c}, A. De Iorio ^{a,b}, F. Fabozzi ^{a,c}, A.O.M. Iorio ^{a,b}, L. Lista ^{a,b,⁵²}, P. Paolucci ^{a,³⁰}, B. Rossi ^a, C. Sciacca ^{a,b}

INFN Sezione di Padova^a, Università di Padova^b, Padova, Italy; Università di Trento^c, Trento, Italy

R. Ardino ^a, P. Azzi ^a, N. Bacchetta ^{a,⁵³}, D. Bisello ^{a,b}, P. Bortignon ^a, A. Bragagnolo ^{a,b}, R. Carlin ^{a,b}, P. Checchia ^a, T. Dorigo ^a, F. Gasparini ^{a,b}, U. Gasparini ^{a,b}, G. Grossi ^a, L. Layer ^{a,⁵⁴}, E. Lusiani ^a, M. Margoni ^{a,b}, A.T. Meneguzzo ^{a,b}, M. Migliorini ^{a,b}, J. Pazzini ^{a,b}, P. Ronchese ^{a,b}, R. Rossin ^{a,b}, F. Simonetto ^{a,b}, G. Strong ^a, M. Tosi ^{a,b}, A. Triossi ^{a,b}, S. Ventura ^a, H. Yasar ^{a,b}, M. Zanetti ^{a,b}, P. Zotto ^{a,b}, A. Zucchetta ^{a,b}, G. Zumerle

INFN Sezione di Pavia^a, Università di Pavia^b, Pavia, Italy

S. Abu Zeid ^{a,⁵⁵}, C. Aimè ^{a,b}, A. Braghieri ^a, S. Calzaferri ^{a,b}, D. Fiorina ^{a,b}, P. Montagna ^{a,b}, V. Re ^a, C. Riccardi ^{a,b}, P. Salvini ^a, I. Vai ^{a,b}, P. Vitulo

INFN Sezione di Perugia^a, Università di Perugia^b, Perugia, Italy

S. Ajmal ^{a,b}, P. Asenov ^{a,⁵⁶}, G.M. Bilei ^a, D. Ciangottini ^{a,b}, L. Fanò ^{a,b}, M. Magherini ^{a,b}, G. Mantovani ^{a,b}, V. Mariani ^{a,b}, M. Menichelli ^a, F. Moscatelli ^{a,⁵⁶}, A. Piccinelli ^{a,b}, M. Presilla ^{a,b}, A. Rossi ^{a,b}, A. Santocchia ^{a,b}, D. Spiga ^a, T. Tedeschi ^{a,b}

INFN Sezione di Pisa^a, Università di Pisa^b, Scuola Normale Superiore di Pisa^c, Pisa, Italy; Università di Siena^d, Siena, Italy

P. Azzurri , G. Bagliesi , R. Bhattacharya , L. Bianchini ^{a,b}, T. Boccali , E. Bossini , D. Bruschini ^{a,c}, R. Castaldi , M.A. Ciocci ^{a,b}, M. Cipriani ^{a,b}, V. D'Amante ^{a,d}, R. Dell'Orso , S. Donato , A. Giassi , F. Ligabue ^{a,c}, D. Matos Figueiredo , A. Messineo ^{a,b}, M. Musich ^{a,b}, F. Palla , S. Parolia , A. Rizzi ^{a,b}, G. Rolandi ^{a,c}, S. Roy Chowdhury , T. Sarkar , A. Scribano , P. Spagnolo , R. Tenchini ^{a,b}, G. Tonelli ^{a,b}, N. Turini ^{a,d}, A. Venturi , P.G. Verdini

INFN Sezione di Roma^a, Sapienza Università di Roma^b, Roma, Italy

P. Barria , M. Campana ^{a,b}, F. Cavallari , L. Cunqueiro Mendez ^{a,b}, D. Del Re ^{a,b}, E. Di Marco , M. Diemoz , F. Errico ^{a,b}, E. Longo ^{a,b}, P. Meridiani , J. Mijuskovic ^{a,b}, G. Organtini ^{a,b}, F. Pandolfi , R. Paramatti ^{a,b}, C. Quaranta ^{a,b}, S. Rahatlou ^{a,b}, C. Rovelli , F. Santanastasio ^{a,b}, L. Soffi , R. Tramontano

INFN Sezione di Torino^a, Università di Torino^b, Torino, Italy; Università del Piemonte Orientale^c, Novara, Italy

N. Amapane ^{a,b}, R. Arcidiacono ^{a,c}, S. Argiro ^{a,b}, M. Arneodo ^{a,c}, N. Bartosik , R. Bellan ^{a,b}, A. Bellora ^{a,b}, C. Biino , N. Cartiglia , M. Costa ^{a,b}, R. Covarelli ^{a,b}, N. Demaria , L. Finco , M. Grippo ^{a,b}, B. Kiani ^{a,b}, F. Legger , F. Luongo ^{a,b}, C. Mariotti , S. Maselli , A. Mecca ^{a,b}, E. Migliore ^{a,b}, M. Monteno , R. Mulargia , M.M. Obertino ^{a,b}, G. Ortona , L. Pacher ^{a,b}, N. Pastrone , M. Pelliccioni , M. Ruspa ^{a,c}, F. Siviero ^{a,b}, V. Sola ^{a,b}, A. Solano ^{a,b}, D. Soldi ^{a,b}, A. Staiano , C. Tarricone ^{a,b}, M. Tornago ^{a,b}, D. Trocino , G. Umoret ^{a,b}, A. Vagnerini ^{a,b}, E. Vlasov

INFN Sezione di Trieste^a, Università di Trieste^b, Trieste, Italy

S. Belforte , V. Candelise ^{a,b}, M. Casarsa , F. Cossutti , K. De Leo ^{a,b}, G. Della Ricca

Kyungpook National University, Daegu, Korea

S. Dogra , J. Hong , C. Huh , B. Kim , D.H. Kim , J. Kim, H. Lee, S.W. Lee , C.S. Moon , Y.D. Oh , S.I. Pak , M.S. Ryu , S. Sekmen , Y.C. Yang

Chonnam National University, Institute for Universe and Elementary Particles, Kwangju, Korea

G. Bak , P. Gwak , H. Kim , D.H. Moon

Hanyang University, Seoul, Korea

E. Asilar , D. Kim , T.J. Kim , J.A. Merlin, J. Park

Korea University, Seoul, Korea

S. Choi , S. Han, B. Hong , K. Lee, K.S. Lee , J. Park, S.K. Park, J. Yoo

Kyung Hee University, Department of Physics, Seoul, Korea

J. Goh

Sejong University, Seoul, KoreaH. S. Kim^{id}, Y. Kim, S. Lee**Seoul National University, Seoul, Korea**J. Almond, J.H. Bhyun, J. Choi^{id}, S. Jeon^{id}, W. Jun^{id}, J. Kim^{id}, J.S. Kim, S. Ko^{id}, H. Kwon^{id}, H. Lee^{id}, J. Lee^{id}, J. Lee^{id}, S. Lee, B.H. Oh^{id}, S.B. Oh^{id}, H. Seo^{id}, U.K. Yang, I. Yoon^{id}**University of Seoul, Seoul, Korea**W. Jang^{id}, D.Y. Kang, Y. Kang^{id}, S. Kim^{id}, B. Ko, J.S.H. Lee^{id}, Y. Lee^{id}, I.C. Park^{id}, Y. Roh, I.J. Watson^{id}, S. Yang^{id}**Yonsei University, Department of Physics, Seoul, Korea**S. Ha^{id}, H.D. Yoo^{id}**Sungkyunkwan University, Suwon, Korea**M. Choi^{id}, M.R. Kim^{id}, H. Lee, Y. Lee^{id}, I. Yu^{id}**College of Engineering and Technology, American University of the Middle East (AUM), Dasman, Kuwait**T. Beyrouty, Y. Maghrbi^{id}**Riga Technical University, Riga, Latvia**K. Dreimanis^{id}, A. Gaile^{id}, G. Pikurs, A. Potrebko^{id}, M. Seidel^{id}, V. Veckalns^{id}⁵⁷**University of Latvia (LU), Riga, Latvia**N.R. Strautnieks^{id}**Vilnius University, Vilnius, Lithuania**M. Ambrozas^{id}, A. Juodagalvis^{id}, A. Rinkevicius^{id}, G. Tamulaitis^{id}**National Centre for Particle Physics, Universiti Malaya, Kuala Lumpur, Malaysia**N. Bin Norjoharuddeen^{id}, I. Yusuff^{id}⁵⁸, Z. Zolkapli**Universidad de Sonora (UNISON), Hermosillo, Mexico**J.F. Benitez^{id}, A. Castaneda Hernandez^{id}, H.A. Encinas Acosta, L.G. Gallegos Maríñez, M. León Coello^{id}, J.A. Murillo Quijada^{id}, A. Sehrawat^{id}, L. Valencia Palomo^{id}**Centro de Investigacion y de Estudios Avanzados del IPN, Mexico City, Mexico**G. Ayala^{id}, H. Castilla-Valdez^{id}, E. De La Cruz-Burelo^{id}, I. Heredia-De La Cruz^{id}⁵⁹, R. Lopez-Fernandez^{id}, C.A. Mondragon Herrera, D.A. Perez Navarro^{id}, A. Sánchez Hernández^{id}**Universidad Iberoamericana, Mexico City, Mexico**C. Oropeza Barrera^{id}, M. Ramírez García^{id}

Benemerita Universidad Autonoma de Puebla, Puebla, MexicoI. Bautista , I. Pedraza , H.A. Salazar Ibarguen , C. Uribe Estrada **University of Montenegro, Podgorica, Montenegro**I. Bubanja, N. Raicevic **University of Canterbury, Christchurch, New Zealand**P.H. Butler **National Centre for Physics, Quaid-I-Azam University, Islamabad, Pakistan**A. Ahmad , M.I. Asghar, A. Awais , M.I.M. Awan, H.R. Hoorani , W.A. Khan **AGH University of Science and Technology Faculty of Computer Science,
Electronics and Telecommunications, Krakow, Poland**V. Avati, L. Grzanka , M. Malawski **National Centre for Nuclear Research, Swierk, Poland**H. Bialkowska , M. Bluj , B. Boimska , M. Górska , M. Kazana , M. Szleper ,
P. Zalewski **Institute of Experimental Physics, Faculty of Physics, University of Warsaw,
Warsaw, Poland**K. Bunkowski , K. Doroba , A. Kalinowski , M. Konecki , J. Krolikowski ,
A. Muhammad **Laboratório de Instrumentação e Física Experimental de Partículas, Lisboa,
Portugal**M. Araujo , D. Bastos , C. Beirão Da Cruz E Silva , A. Boletti , M. Bozzo , P. Faccioli ,
M. Gallinaro , J. Hollar , N. Leonardo , T. Niknejad , M. Pisano , J. Seixas , J. Varela **Faculty of Physics, University of Belgrade, Belgrade, Serbia**P. Adzic , P. Milenovic **VINCA Institute of Nuclear Sciences, University of Belgrade, Belgrade,
Serbia**M. Dordevic , J. Milosevic , V. Rekovic**Centro de Investigaciones Energéticas Medioambientales y Tecnológicas
(CIEMAT), Madrid, Spain**M. Aguilar-Benitez, J. Alcaraz Maestre , M. Barrio Luna, Cristina F. Bedoya , M. Cepeda ,
M. Cerrada , N. Colino , B. De La Cruz , A. Delgado Peris , D. Fernández Del Val ,
J.P. Fernández Ramos , J. Flix , M.C. Fouz , O. Gonzalez Lopez , S. Goy Lopez ,
J.M. Hernandez , M.I. Josa , J. León Holgado , D. Moran , C. M. Morcillo Perez ,
Á. Navarro Tobar , C. Perez Dengra , A. Pérez-Calero Yzquierdo , J. Puerta Pelayo ,
I. Redondo , D.D. Redondo Ferrero , L. Romero, S. Sánchez Navas , L. Urda Gómez ,
J. Vazquez Escobar , C. Willmott

Universidad Autónoma de Madrid, Madrid, SpainJ.F. de Trocóniz **Universidad de Oviedo, Instituto Universitario de Ciencias y Tecnologías Espaciales de Asturias (ICTEA), Oviedo, Spain**

B. Alvarez Gonzalez , J. Cuevas , J. Fernandez Menendez , S. Folgueras ,
 I. Gonzalez Caballero , J.R. González Fernández , E. Palencia Cortezon ,
 C. Ramón Álvarez , V. Rodríguez Bouza , A. Soto Rodríguez , A. Trapote ,
 C. Vico Villalba , P. Vischia 

Instituto de Física de Cantabria (IFCA), CSIC-Universidad de Cantabria, Santander, Spain

S. Bhowmik , S. Blanco Fernández , J.A. Brochero Cifuentes , I.J. Cabrillo , A. Calderon ,
 J. Duarte Campderros , M. Fernandez , C. Fernandez Madrazo , G. Gomez ,
 C. Lasaosa García , C. Martinez Rivero , P. Martinez Ruiz del Arbol , F. Matorras ,
 P. Matorras Cuevas , E. Navarrete Ramos , J. Piedra Gomez , C. Prieels, L. Scodelaro ,
 I. Vila , J.M. Vizan Garcia 

University of Colombo, Colombo, Sri LankaM.K. Jayananda , B. Kailasapathy ⁶⁰, D.U.J. Sonnadara , D.D.C. Wickramarathna **University of Ruhuna, Department of Physics, Matara, Sri Lanka**W.G.D. Dharmaratna , K. Liyanage , N. Perera , N. Wickramage **CERN, European Organization for Nuclear Research, Geneva, Switzerland**

D. Abbaneo , C. Amendola , E. Auffray , G. Auzinger , J. Baechler, D. Barney ,
 A. Bermúdez Martínez , M. Bianco , B. Bilin , A.A. Bin Anuar , A. Bocci ,
 E. Brondolin , C. Caillol , T. Camporesi , G. Cerminara , N. Chernyavskaya ,
 D. d'Enterria , A. Dabrowski , A. David , A. De Roeck , M.M. Defranchis , M. Deile ,
 M. Dobson , F. Fallavollita ⁶¹, L. Forthomme , G. Franzoni , W. Funk , S. Giani, D. Gigi,
 K. Gill , F. Glege , L. Gouskos , M. Haranko , J. Hegeman , V. Innocente , T. James ,
 P. Janot , J. Kieseler , S. Laurila , P. Lecoq , E. Leutgeb , C. Lourenço , B. Maier ,
 L. Malgeri , M. Mannelli , A.C. Marini , F. Meijers , S. Mersi , E. Meschi ,
 V. Milosevic , F. Moortgat , M. Mulders , S. Orfanelli, F. Pantaleo , M. Peruzzi ,
 A. Petrilli , G. Petrucciani , A. Pfeiffer , M. Pierini , D. Piparo , H. Qu , D. Rabady ,
 G. Reales Gutiérrez, M. Rovere , H. Sakulin , S. Scarfi , M. Selvaggi , A. Sharma ,
 K. Shchelina , P. Silva , P. Sphicas ⁶², A.G. Stahl Leiton , A. Steen , S. Summers ,
 D. Treille , P. Tropea , A. Tsirou, D. Walter , J. Wanzyk ⁶³, K.A. Wozniak ⁶⁴,
 P. Zehetner , P. Zejdl , W.D. Zeuner

Paul Scherrer Institut, Villigen, Switzerland

T. Bevilacqua , L. Caminada ⁶⁵, A. Ebrahimi , W. Erdmann , R. Horisberger ,
 Q. Ingram , H.C. Kaestli , D. Kotlinski , C. Lange , M. Missiroli ⁶⁵, L. Noehte ⁶⁵,
 T. Rohe 

ETH Zurich — Institute for Particle Physics and Astrophysics (IPA), Zurich, Switzerland

T.K. Aarrestad , K. Androsov ⁶³, M. Backhaus , A. Calandri , C. Cazzaniga , K. Datta , A. De Cosa , G. Dissertori , M. Dittmar, M. Donegà , F. Eble , M. Galli , K. Gedia , F. Glessgen , C. Grab , D. Hits , W. Lustermann , A.-M. Lyon , R.A. Manzoni , M. Marchegiani , L. Marchese , C. Martin Perez , A. Mascellani ⁶³, F. Nesi-Tedaldi , F. Pauss , V. Perovic , S. Pigazzini , M.G. Ratti , M. Reichmann , C. Reissel , T. Reitenspiess , B. Ristic , F. Riti , D. Ruini, D.A. Sanz Becerra , R. Seidita , J. Steggemann ⁶³, D. Valsecchi , R. Wallny

Universität Zürich, Zurich, Switzerland

C. Amsler ⁶⁶, P. Bärtschi , C. Botta , D. Brzhechko, M.F. Canelli , K. Cormier , A. De Wit , R. Del Burgo, J.K. Heikkilä , M. Huwiler , W. Jin , A. Jofrehei , B. Kilminster , S. Leontsinis , S.P. Liechti , A. Macchiolo , P. Meiring , V.M. Mikuni , U. Molinatti , I. Neutelings , A. Reimers , P. Robmann, S. Sanchez Cruz , K. Schweiger , M. Senger , Y. Takahashi

National Central University, Chung-Li, Taiwan

C. Adloff ⁶⁷, C.M. Kuo, W. Lin, P.K. Rout , P.C. Tiwari ⁴¹, S.S. Yu

National Taiwan University (NTU), Taipei, Taiwan

L. Ceard, Y. Chao , K.F. Chen , P.s. Chen, Z.g. Chen, W.-S. Hou , T.h. Hsu, Y.w. Kao, R. Khurana, G. Kole , Y.y. Li , R.-S. Lu , E. Paganis , A. Psallidas, X.f. Su, J. Thomas-Wilsker , H.y. Wu, E. Yazgan

Chulalongkorn University, Faculty of Science, Department of Physics, Bangkok, Thailand

C. Asawatangtrakuldee , N. Srimanobhas , V. Wachirapusanand

Çukurova University, Physics Department, Science and Art Faculty, Adana, Turkey

D. Agyel , F. Boran , Z.S. Demiroglu , F. Dolek , I. Dumanoglu ⁶⁸, E. Eskut , Y. Guler ⁶⁹, E. Gurpinar Guler ⁶⁹, C. Isik , O. Kara, A. Kayis Topaksu , U. Kiminsu , G. Onengut , K. Ozdemir ⁷⁰, A. Polatoz , B. Tali ⁷¹, U.G. Tok , S. Turkcapar , E. Uslan , I.S. Zorbakir

Middle East Technical University, Physics Department, Ankara, Turkey

K. Ocalan ⁷², M. Yalvac ⁷³

Bogazici University, Istanbul, Turkey

B. Akgun , I.O. Atakisi , E. Gülmmez , M. Kaya ⁷⁴, O. Kaya ⁷⁵, S. Tekten ⁷⁶

Istanbul Technical University, Istanbul, Turkey

A. Cakir , K. Cankocak ⁶⁸, Y. Komurcu , S. Sen ⁷⁷

Istanbul University, Istanbul, Turkey

O. Aydilek , S. Cerci ⁷¹, V. Epshteyn , B. Hacisahinoglu , I. Hos ⁷⁸, B. Isildak ⁷⁹,
B. Kaynak , S. Ozkorucuklu , H. Sert , C. Simsek , D. Sunar Cerci ⁷¹, C. Zorbilmez

Institute for Scintillation Materials of National Academy of Science of Ukraine, Kharkiv, Ukraine

A. Boyaryntsev , B. Grynyov 

National Science Centre, Kharkiv Institute of Physics and Technology, Kharkiv, Ukraine

L. Levchuk 

University of Bristol, Bristol, United Kingdom

D. Anthony , J.J. Brooke , A. Bundock , F. Bury , E. Clement , D. Cussans ,
H. Flacher , M. Glowacki, J. Goldstein , H.F. Heath , L. Kreczko , B. Krikler ,
S. Paramesvaran , S. Seif El Nasr-Storey, V.J. Smith , N. Stylianou ⁸⁰, K. Walkingshaw Pass,
R. White

Rutherford Appleton Laboratory, Didcot, United Kingdom

A.H. Ball, K.W. Bell , A. Belyaev ⁸¹, C. Brew , R.M. Brown , D.J.A. Cockerill ,
C. Cooke , K.V. Ellis, K. Harder , S. Harper , M.-L. Holmberg ⁸², Sh. Jain , J. Linacre ,
K. Manolopoulos, D.M. Newbold , E. Olaiya, D. Petyt , T. Reis , G. Salvi , T. Schuh,
C.H. Shepherd-Themistocleous , I.R. Tomalin , T. Williams

Imperial College, London, United Kingdom

R. Bainbridge , P. Bloch , C.E. Brown , O. Buchmuller, V. Cacchio,
C.A. Carrillo Montoya , G.S. Chahal ⁸³, D. Colling , J.S. Dancu, P. Dauncey , G. Davies ,
J. Davies, M. Della Negra , S. Fayer, G. Fedi , G. Hall , M.H. Hassanshahi , A. Howard,
G. Iles , M. Knight , J. Langford , L. Lyons , A.-M. Magnan , S. Malik, A. Martelli ,
M. Mieskolainen , J. Nash ⁸⁴, M. Pesaresi, B.C. Radburn-Smith , A. Richards, A. Rose ,
C. Seez , R. Shukla , A. Tapper , K. Uchida , G.P. Uttley , L.H. Vage, T. Virdee ³⁰,
M. Vojinovic , N. Wardle , D. Winterbottom

Brunel University, Uxbridge, United Kingdom

K. Coldham, J.E. Cole , A. Khan, P. Kyberd , I.D. Reid 

Baylor University, Waco, Texas, U.S.A.

S. Abdullin , A. Brinkerhoff , B. Caraway , J. Dittmann , K. Hatakeyama ,
J. Hiltbrand , A.R. Kanuganti , B. McMaster , M. Saunders , S. Sawant ,
C. Sutantawibul , M. Toms ⁸⁵, J. Wilson

Catholic University of America, Washington, DC, U.S.A.

R. Bartek , A. Dominguez , C. Huerta Escamilla, A.E. Simsek , R. Uniyal ,
A.M. Vargas Hernandez 

The University of Alabama, Tuscaloosa, Alabama, U.S.A.

R. Chudasama^{ID}, S.I. Cooper^{ID}, S.V. Gleyzer^{ID}, C.U. Perez^{ID}, P. Rumerio^{ID}⁸⁶, E. Usai^{ID}, C. West^{ID}, R. Yi^{ID}

Boston University, Boston, Massachusetts, U.S.A.

A. Akpinar^{ID}, A. Albert^{ID}, D. Arcaro^{ID}, C. Cosby^{ID}, Z. Demiragli^{ID}, C. Erice^{ID}, E. Fontanesi^{ID}, D. Gastler^{ID}, J. Rohlf^{ID}, K. Salyer^{ID}, D. Sperka^{ID}, D. Spitzbart^{ID}, I. Suarez^{ID}, A. Tsatsos^{ID}, S. Yuan^{ID}

Brown University, Providence, Rhode Island, U.S.A.

G. Benelli^{ID}, X. Coubez²⁵, D. Cutts^{ID}, M. Hadley^{ID}, U. Heintz^{ID}, J.M. Hogan^{ID}⁸⁷, T. Kwon^{ID}, G. Landsberg^{ID}, K.T. Lau^{ID}, D. Li^{ID}, J. Luo^{ID}, S. Mondal^{ID}, M. Narain^{ID}[†], N. Pervan^{ID}, S. Sagir^{ID}⁸⁸, F. Simpson^{ID}, W.Y. Wong, X. Yan^{ID}, W. Zhang

University of California, Davis, Davis, California, U.S.A.

S. Abbott^{ID}, J. Bonilla^{ID}, C. Brainerd^{ID}, R. Breedon^{ID}, M. Calderon De La Barca Sanchez^{ID}, M. Chertok^{ID}, M. Citron^{ID}, J. Conway^{ID}, P.T. Cox^{ID}, R. Erbacher^{ID}, G. Haza^{ID}, F. Jensen^{ID}, O. Kukral^{ID}, G. Mocellin^{ID}, M. Mulhearn^{ID}, D. Pellett^{ID}, B. Regnery^{ID}, W. Wei^{ID}, Y. Yao^{ID}, F. Zhang^{ID}

University of California, Los Angeles, California, U.S.A.

M. Bachtis^{ID}, R. Cousins^{ID}, A. Datta^{ID}, J. Hauser^{ID}, M. Ignatenko^{ID}, M.A. Iqbal^{ID}, T. Lam^{ID}, E. Manca^{ID}, W.A. Nash^{ID}, D. Saltzberg^{ID}, B. Stone^{ID}, V. Valuev^{ID}

University of California, Riverside, Riverside, California, U.S.A.

R. Clare^{ID}, M. Gordon, G. Hanson^{ID}, W. Si^{ID}, S. Wimpenny^{ID}[†]

University of California, San Diego, La Jolla, California, U.S.A.

J.G. Branson^{ID}, S. Cittolin^{ID}, S. Cooperstein^{ID}, D. Diaz^{ID}, J. Duarte^{ID}, R. Gerosa^{ID}, L. Giannini^{ID}, J. Guiang^{ID}, R. Kansal^{ID}, V. Krutelyov^{ID}, R. Lee^{ID}, J. Letts^{ID}, M. Masciovecchio^{ID}, F. Mokhtar^{ID}, M. Pieri^{ID}, M. Quinnan^{ID}, B.V. Sathia Narayanan^{ID}, V. Sharma^{ID}, M. Tadel^{ID}, E. Vourliotis^{ID}, F. Würthwein^{ID}, Y. Xiang^{ID}, A. Yagil^{ID}

University of California, Santa Barbara — Department of Physics, Santa Barbara, California, U.S.A.

L. Brennan, C. Campagnari^{ID}, G. Collura^{ID}, A. Dorsett^{ID}, J. Incandela^{ID}, M. Kilpatrick^{ID}, J. Kim^{ID}, A.J. Li^{ID}, P. Masterson^{ID}, H. Mei^{ID}, M. Oshiro^{ID}, J. Richman^{ID}, U. Sarica^{ID}, R. Schmitz^{ID}, F. Setti^{ID}, J. Sheplock^{ID}, D. Stuart^{ID}, S. Wang^{ID}

California Institute of Technology, Pasadena, California, U.S.A.

A. Bornheim^{ID}, O. Cerri, A. Latorre, J.M. Lawhorn^{ID}, J. Mao^{ID}, H.B. Newman^{ID}, T. Q. Nguyen^{ID}, M. Spiropulu^{ID}, J.R. Vlimant^{ID}, C. Wang^{ID}, S. Xie^{ID}, R.Y. Zhu^{ID}

Carnegie Mellon University, Pittsburgh, Pennsylvania, U.S.A.

J. Alison^{ID}, S. An^{ID}, M.B. Andrews^{ID}, P. Bryant^{ID}, V. Dutta^{ID}, T. Ferguson^{ID}, A. Harilal^{ID}, C. Liu^{ID}, T. Mudholkar^{ID}, S. Murthy^{ID}, M. Paulini^{ID}, A. Roberts^{ID}, A. Sanchez^{ID}, W. Terrill^{ID}

University of Colorado Boulder, Boulder, Colorado, U.S.A.

J.P. Cumalat , W.T. Ford , A. Hassani , G. Karathanasis , E. MacDonald, N. Manganelli , F. Marini , A. Perloff , C. Savard , N. Schonbeck , K. Stenson , K.A. Ulmer , S.R. Wagner , N. Zipper

Cornell University, Ithaca, New York, U.S.A.

J. Alexander , S. Bright-Thonney , X. Chen , D.J. Cranshaw , J. Fan , X. Fan , D. Gadkari , S. Hogan , J. Monroy , J.R. Patterson , J. Reichert , M. Reid , A. Ryd , J. Thom , P. Wittich , R. Zou

Fermi National Accelerator Laboratory, Batavia, Illinois, U.S.A.

M. Albrow , M. Alyari , O. Amram , G. Apollinari , A. Apresyan , L.A.T. Bauer , D. Berry , J. Berryhill , P.C. Bhat , K. Burkett , J.N. Butler , A. Canepa , G.B. Cerati , H.W.K. Cheung , F. Chlebana , G. Cummings , J. Dickinson , I. Dutta , V.D. Elvira , Y. Feng , J. Freeman , A. Gandrakota , Z. Gecse , L. Gray , D. Green, S. Grünendahl , D. Guerrero , O. Gutsche , R.M. Harris , R. Heller , T.C. Herwig , J. Hirschauer , L. Horyn , B. Jayatilaka , S. Jindariani , M. Johnson , U. Joshi , T. Klijnsma , B. Klima , K.H.M. Kwok , S. Lammel , D. Lincoln , R. Lipton , T. Liu , C. Madrid , K. Maeshima , C. Mantilla , D. Mason , P. McBride , P. Merkel , S. Mrenna , S. Nahm , J. Ngadiuba , D. Noonan , V. Papadimitriou , N. Pastika , K. Pedro , C. Pena ⁸⁹, F. Ravera , A. Reinsvold Hall ⁹⁰, L. Ristori , E. Sexton-Kennedy , N. Smith , A. Soha , L. Spiegel , S. Stoynev , L. Taylor , S. Tkaczyk , N.V. Tran , L. Uplegger , E.W. Vaandering , I. Zoi

University of Florida, Gainesville, Florida, U.S.A.

C. Aruta , P. Avery , D. Bourilkov , L. Cadamuro , P. Chang , V. Cherepanov , R.D. Field, E. Koenig , M. Kolosova , J. Konigsberg , A. Korytov , K.H. Lo, K. Matchev , N. Menendez , G. Mitselmakher , A. Muthirakalayil Madhu , N. Rawal , D. Rosenzweig , S. Rosenzweig , K. Shi , J. Wang

Florida State University, Tallahassee, Florida, U.S.A.

T. Adams , A. Al Kadhim , A. Askew , N. Bower , R. Habibullah , V. Hagopian , R. Hashmi , R.S. Kim , S. Kim , T. Kolberg , G. Martinez, H. Prosper , P.R. Prova, O. Viazlo , M. Wulansatiti , R. Yohay , J. Zhang

Florida Institute of Technology, Melbourne, Florida, U.S.A.

B. Alsufyani, M.M. Baarmand , S. Butalla , T. Elkafrawy ⁵⁵, M. Hohlmann , R. Kumar Verma , M. Rahmani, F. Yumiceva

University of Illinois at Chicago (UIC), Chicago, Illinois, U.S.A.

M.R. Adams , C. Bennett, R. Cavanaugh , S. Dittmer , R. Escobar Franco , O. Evdokimov , C.E. Gerber , D.J. Hofman , J.h. Lee , D. S. Lemos , A.H. Merrit , C. Mills , S. Nanda , G. Oh , B. Ozek , D. Pilipovic , T. Roy , S. Rudrabhatla , M.B. Tonjes , N. Varelas , X. Wang , Z. Ye , J. Yoo

The University of Iowa, Iowa City, Iowa, U.S.A.

M. Alhusseini , D. Blend, K. Dilsiz 91, L. Emediato , G. Karaman , O.K. Köseyan , J.-P. Merlo, A. Mestvirishvili 92, J. Nachtman , O. Neogi, H. Ogul 93, Y. Onel , A. Penzo , C. Snyder, E. Tiras 94

Johns Hopkins University, Baltimore, Maryland, U.S.A.

B. Blumenfeld , L. Corcodilos , J. Davis , A.V. Gritsan , L. Kang , S. Kyriacou , P. Maksimovic , M. Roguljic , J. Roskes , S. Sekhar , M. Swartz , T.Á. Vámi

The University of Kansas, Lawrence, Kansas, U.S.A.

A. Abreu , L.F. Alcerro Alcerro , J. Anguiano , P. Baringer , A. Bean , Z. Flowers , D. Grove, J. King , G. Krintiras , M. Lazarovits , C. Le Mahieu , C. Lindsey, J. Marquez , N. Minafra , M. Murray , M. Nickel , M. Pitt , S. Popescu 95, C. Rogan , C. Royon , R. Salvatico , S. Sanders , C. Smith , Q. Wang , G. Wilson

Kansas State University, Manhattan, Kansas, U.S.A.

B. Allmond , A. Ivanov , K. Kaadze , A. Kalogeropoulos , D. Kim, Y. Maravin , K. Nam, J. Natoli , D. Roy , G. Sorrentino

Lawrence Livermore National Laboratory, Livermore, California, U.S.A.

F. Rebassoo , D. Wright

University of Maryland, College Park, Maryland, U.S.A.

E. Adams , A. Baden , O. Baron, A. Belloni , A. Bethani , Y.M. Chen , S.C. Eno , N.J. Hadley , S. Jabeen , R.G. Kellogg , T. Koeth , Y. Lai , S. Lascio , A.C. Mignerey , S. Nabili , C. Palmer , C. Papageorgakis , M.M. Paranjpe, L. Wang , K. Wong

Massachusetts Institute of Technology, Cambridge, Massachusetts, U.S.A.

J. Bendavid , W. Busza , I.A. Cali , Y. Chen , M. D'Alfonso , J. Eysermans , C. Freer , G. Gomez-Ceballos , M. Goncharov, P. Harris, D. Hoang, D. Kovalskyi , J. Krupa , L. Lavezzo , Y.-J. Lee , K. Long , C. Mironov , C. Paus , D. Rankin , C. Roland , G. Roland , S. Rothman , Z. Shi , G.S.F. Stephans , J. Wang, Z. Wang , B. Wyslouch , T. J. Yang

University of Minnesota, Minneapolis, Minnesota, U.S.A.

B. Crossman , B.M. Joshi , C. Kapsiak , M. Krohn , D. Mahon , J. Mans , B. Marzocchi , S. Pandey , M. Revering , R. Rusack , R. Saradhy , N. Schroeder , N. Strobbe , M.A. Wadud

University of Mississippi, Oxford, Mississippi, U.S.A.

L.M. Cremaldi

University of Nebraska-Lincoln, Lincoln, Nebraska, U.S.A.

K. Bloom , M. Bryson, D.R. Claes , C. Fangmeier , F. Golf , J. Hossain , C. Joo , I. Kravchenko , I. Reed , J.E. Siado , G.R. Snow[†], W. Tabb , A. Wightman , F. Yan , D. Yu , A.G. Zecchinelli

State University of New York at Buffalo, Buffalo, New York, U.S.A.

G. Agarwal¹⁰, H. Bandyopadhyay¹⁰, L. Hay¹⁰, I. Iashvili¹⁰, A. Kharchilava¹⁰, C. McLean¹⁰, M. Morris¹⁰, D. Nguyen¹⁰, J. Pekkanen¹⁰, S. Rappoccio¹⁰, H. Rejeb Sfar, A. Williams¹⁰

Northeastern University, Boston, Massachusetts, U.S.A.

G. Alverson¹⁰, E. Barberis¹⁰, Y. Haddad¹⁰, Y. Han¹⁰, A. Krishna¹⁰, J. Li¹⁰, M. Lu¹⁰, G. Madigan¹⁰, D.M. Morse¹⁰, V. Nguyen¹⁰, T. Orimoto¹⁰, A. Parker¹⁰, L. Skinnari¹⁰, A. Tishelman-Charny¹⁰, B. Wang¹⁰, D. Wood¹⁰

Northwestern University, Evanston, Illinois, U.S.A.

S. Bhattacharya¹⁰, J. Bueghly, Z. Chen¹⁰, K.A. Hahn¹⁰, Y. Liu¹⁰, Y. Miao¹⁰, D.G. Monk¹⁰, M.H. Schmitt¹⁰, A. Taliercio¹⁰, M. Velasco

University of Notre Dame, Notre Dame, Indiana, U.S.A.

R. Band¹⁰, R. Bucci, S. Castells¹⁰, M. Cremonesi, A. Das¹⁰, R. Goldouzian¹⁰, M. Hildreth¹⁰, K.W. Ho¹⁰, K. Hurtado Anampa¹⁰, C. Jessop¹⁰, K. Lannon¹⁰, J. Lawrence¹⁰, N. Loukas¹⁰, L. Lutton¹⁰, J. Mariano, N. Marinelli, I. Mcalister, T. McCauley¹⁰, C. Mcgrady¹⁰, K. Mohrman¹⁰, C. Moore¹⁰, Y. Musienko¹⁰¹³, H. Nelson¹⁰, M. Osherson¹⁰, R. Ruchti¹⁰, A. Townsend¹⁰, M. Wayne¹⁰, H. Yockey, M. Zarucki¹⁰, L. Zygalas¹⁰

The Ohio State University, Columbus, Ohio, U.S.A.

A. Basnet¹⁰, B. Bylsma, M. Carrigan¹⁰, L.S. Durkin¹⁰, C. Hill¹⁰, M. Joyce¹⁰, A. Lesauvage¹⁰, M. Nunez Ornelas¹⁰, K. Wei, B.L. Winer¹⁰, B. R. Yates¹⁰

Princeton University, Princeton, New Jersey, U.S.A.

F.M. Addesa¹⁰, H. Bouchamaoui¹⁰, P. Das¹⁰, G. Dezoort¹⁰, P. Elmer¹⁰, A. Frankenthal¹⁰, B. Greenberg¹⁰, N. Haubrich¹⁰, S. Higginbotham¹⁰, G. Kopp¹⁰, S. Kwan¹⁰, D. Lange¹⁰, A. Loeliger¹⁰, D. Marlow¹⁰, I. Ojalvo¹⁰, J. Olsen¹⁰, D. Stickland¹⁰, C. Tully¹⁰

University of Puerto Rico, Mayaguez, Puerto Rico, U.S.A.

S. Malik¹⁰

Purdue University, West Lafayette, Indiana, U.S.A.

A.S. Bakshi¹⁰, V.E. Barnes¹⁰, S. Chandra¹⁰, R. Chawla¹⁰, S. Das¹⁰, A. Gu¹⁰, L. Gutay, M. Jones¹⁰, A.W. Jung¹⁰, D. Kondratyev¹⁰, A.M. Koshy, M. Liu¹⁰, G. Negro¹⁰, N. Neumeister¹⁰, G. Paspalaki¹⁰, S. Piperov¹⁰, A. Purohit¹⁰, J.F. Schulte¹⁰, M. Stojanovic¹⁰, J. Thieman¹⁰, A. K. Virdi¹⁰, F. Wang¹⁰, W. Xie¹⁰

Purdue University Northwest, Hammond, Indiana, U.S.A.

J. Dolen¹⁰, N. Parashar¹⁰, A. Pathak¹⁰

Rice University, Houston, Texas, U.S.A.

D. Acosta¹⁰, A. Baty¹⁰, T. Carnahan¹⁰, S. Dildick¹⁰, K.M. Ecklund¹⁰, P.J. Fernández Manteca¹⁰, S. Freed, P. Gardner, F.J.M. Geurts¹⁰, A. Kumar¹⁰, W. Li¹⁰, O. Miguel Colin¹⁰, B.P. Padley¹⁰, R. Redjimi, J. Rotter¹⁰, E. Yigitbasi¹⁰, Y. Zhang¹⁰

University of Rochester, Rochester, New York, U.S.A.

- A. Bodek , P. de Barbaro , R. Demina , J.L. Dulemba , C. Fallon, A. Garcia-Bellido , O. Hindrichs , A. Khukhunaishvili , P. Parygin ⁸⁵, E. Popova ⁸⁵, R. Taus , G.P. Van Onsem 

The Rockefeller University, New York, New York, U.S.A.

- K. Goulianatos 

Rutgers, The State University of New Jersey, Piscataway, New Jersey, U.S.A.

- B. Chiarito, J.P. Chou , Y. Gershtein , E. Halkiadakis , A. Hart , M. Heindl , D. Jaroslawski , O. Karacheban ²⁸, I. Laflotte , A. Lath , R. Montalvo, K. Nash, H. Routray , S. Salur , S. Schnetzer, S. Somalwar , R. Stone , S.A. Thayil , S. Thomas, J. Vora , H. Wang

University of Tennessee, Knoxville, Tennessee, U.S.A.

- H. Acharya, D. Ally , A.G. Delannoy , S. Fiorendi , T. Holmes , N. Karunarathna , L. Lee , E. Nibigira , S. Spanier 

Texas A&M University, College Station, Texas, U.S.A.

- D. Aebi , M. Ahmad , O. Bouhali ⁹⁶, M. Dalchenko , R. Eusebi , J. Gilmore , T. Huang , T. Kamon ⁹⁷, H. Kim , S. Luo , S. Malhotra, R. Mueller , D. Overton , D. Rathjens , A. Safonov

Texas Tech University, Lubbock, Texas, U.S.A.

- N. Akchurin , J. Damgov , V. Hegde , A. Hussain , Y. Kazhykarim, K. Lamichhane , S.W. Lee , A. Mankel , T. Mengke, S. Muthumuni , T. Peltola , I. Volobouev , A. Whitbeck 

Vanderbilt University, Nashville, Tennessee, U.S.A.

- E. Appelt , S. Greene, A. Gurrola , W. Johns , R. Kunnavalkam Elayavalli , A. Melo , F. Romeo , P. Sheldon , S. Tuo , J. Velkovska , J. Viinikainen 

University of Virginia, Charlottesville, Virginia, U.S.A.

- B. Cardwell , B. Cox , J. Hakala , R. Hirosky , A. Ledovskoy , A. Li , C. Neu , C.E. Perez Lara 

Wayne State University, Detroit, Michigan, U.S.A.

- P.E. Karchin 

University of Wisconsin — Madison, Madison, Wisconsin, U.S.A.

- A. Aravind, S. Banerjee , K. Black , T. Bose , S. Dasu , I. De Bruyn , P. Everaerts , C. Galloni, H. He , M. Herndon , A. Herve , C.K. Koraka , A. Lanaro, R. Loveless , J. Madhusudanan Sreekala , A. Mallampalli , A. Mohammadi , S. Mondal, G. Parida , D. Pinna, A. Savin, V. Shang , V. Sharma , W.H. Smith , D. Teague, H.F. Tsoi , W. Vetens , A. Warden

Authors affiliated with an institute or an international laboratory covered by a cooperation agreement with CERN

S. Afanasiev^{ID}, V. Andreev^{ID}, Yu. Andreev^{ID}, T. Aushev^{ID}, M. Azarkin^{ID}, A. Babaev^{ID}, A. Belyaev^{ID}, V. Blinov⁹⁸, E. Boos^{ID}, V. Borshch^{ID}, D. Budkouski^{ID}, M. Chadeeva^{ID}⁹⁸, V. Chekhovsky, A. Dermenev^{ID}, T. Dimova^{ID}⁹⁸, D. Druzhkin^{ID}⁹⁹, M. Dubinin^{ID}⁸⁹, L. Dudko^{ID}, A. Ershov^{ID}, G. Gavrilov^{ID}, V. Gavrilov^{ID}, S. Gnninenko^{ID}, V. Golovtcov^{ID}, N. Golubev^{ID}, I. Golutvin^{ID}, I. Gorbunov^{ID}, A. Gribushin^{ID}, Y. Ivanov^{ID}, V. Kachanov^{ID}, L. Kardapoltsev^{ID}⁹⁸, V. Karjavine^{ID}, A. Karneyeu^{ID}, V. Kim^{ID}⁹⁸, M. Kirakosyan, D. Kirpichnikov^{ID}, M. Kirsanov^{ID}, V. Klyukhin^{ID}, O. Kodolova^{ID}¹⁰⁰, D. Konstantinov^{ID}, V. Korenkov^{ID}, A. Kozyrev^{ID}⁹⁸, N. Krasnikov^{ID}, A. Lanev^{ID}, P. Levchenko^{ID}¹⁰¹, N. Lychkovskaya^{ID}, V. Makarenko^{ID}, A. Malakhov^{ID}, V. Matveev^{ID}⁹⁸, V. Murzin^{ID}, A. Nikitenko^{ID}^{102,100}, S. Obraztsov^{ID}, V. Oreshkin^{ID}, V. Palichik^{ID}, V. Perelygin^{ID}, S. Petrushanko^{ID}, S. Polikarpov^{ID}⁹⁸, V. Popov, O. Radchenko^{ID}⁹⁸, V. Rusinov, M. Savina^{ID}, V. Savrin^{ID}, D. Selivanova^{ID}, V. Shalaev^{ID}, S. Shmatov^{ID}, S. Shulha^{ID}, Y. Skovpen^{ID}⁹⁸, S. Slabospitskii^{ID}, V. Smirnov^{ID}, A. Snigirev^{ID}, D. Sosnov^{ID}, V. Sulimov^{ID}, E. Tcherniaev^{ID}, A. Terkulov^{ID}, O. Teryaev^{ID}, I. Tlisova^{ID}, A. Toropin^{ID}, L. Uvarov^{ID}, A. Uzunian^{ID}, A. Vorobyev[†], N. Voigtishin^{ID}, B.S. Yuldashev¹⁰³, A. Zarubin^{ID}, I. Zhizhin^{ID}, A. Zhokin^{ID}

[†] Deceased

¹ Also at Yerevan State University, Yerevan, Armenia

² Also at TU Wien, Vienna, Austria

³ Also at Institute of Basic and Applied Sciences, Faculty of Engineering, Arab Academy for Science, Technology and Maritime Transport, Alexandria, Egypt

⁴ Also at Ghent University, Ghent, Belgium

⁵ Also at Universidade Estadual de Campinas, Campinas, Brazil

⁶ Also at Federal University of Rio Grande do Sul, Porto Alegre, Brazil

⁷ Also at UFMS, Nova Andradina, Brazil

⁸ Also at Nanjing Normal University, Nanjing, China

⁹ Now at The University of Iowa, Iowa City, Iowa, U.S.A.

¹⁰ Also at University of Chinese Academy of Sciences, Beijing, China

¹¹ Also at University of Chinese Academy of Sciences, Beijing, China

¹² Also at Université Libre de Bruxelles, Bruxelles, Belgium

¹³ Also at an institute or an international laboratory covered by a cooperation agreement with CERN

¹⁴ Also at Cairo University, Cairo, Egypt

¹⁵ Also at Suez University, Suez, Egypt

¹⁶ Now at British University in Egypt, Cairo, Egypt

¹⁷ Also at Birla Institute of Technology, Mesra, Mesra, India

¹⁸ Also at Purdue University, West Lafayette, Indiana, U.S.A.

¹⁹ Also at Université de Haute Alsace, Mulhouse, France

²⁰ Also at Department of Physics, Tsinghua University, Beijing, China

²¹ Also at Tbilisi State University, Tbilisi, Georgia

²² Also at The University of the State of Amazonas, Manaus, Brazil

²³ Also at Erzincan Binali Yildirim University, Erzincan, Turkey

²⁴ Also at University of Hamburg, Hamburg, Germany

²⁵ Also at RWTH Aachen University, III. Physikalisches Institut A, Aachen, Germany

²⁶ Also at Isfahan University of Technology, Isfahan, Iran

²⁷ Also at Bergische University Wuppertal (BUW), Wuppertal, Germany

²⁸ Also at Brandenburg University of Technology, Cottbus, Germany

²⁹ Also at Forschungszentrum Jülich, Juelich, Germany

- ³⁰ Also at CERN, European Organization for Nuclear Research, Geneva, Switzerland
³¹ Also at Physics Department, Faculty of Science, Assiut University, Assiut, Egypt
³² Also at Wigner Research Centre for Physics, Budapest, Hungary
³³ Also at Institute of Physics, University of Debrecen, Debrecen, Hungary
³⁴ Also at Institute of Nuclear Research ATOMKI, Debrecen, Hungary
³⁵ Now at Universitatea Babes-Bolyai — Facultatea de Fizica, Cluj-Napoca, Romania
³⁶ Also at Faculty of Informatics, University of Debrecen, Debrecen, Hungary
³⁷ Also at Punjab Agricultural University, Ludhiana, India
³⁸ Also at UPES — University of Petroleum and Energy Studies, Dehradun, India
³⁹ Also at University of Visva-Bharati, Santiniketan, India
⁴⁰ Also at University of Hyderabad, Hyderabad, India
⁴¹ Also at Indian Institute of Science (IISc), Bangalore, India
⁴² Also at IIT Bhubaneswar, Bhubaneswar, India
⁴³ Also at Institute of Physics, Bhubaneswar, India
⁴⁴ Also at Deutsches Elektronen-Synchrotron, Hamburg, Germany
⁴⁵ Also at Department of Physics, Isfahan University of Technology, Isfahan, Iran
⁴⁶ Also at Sharif University of Technology, Tehran, Iran
⁴⁷ Also at Department of Physics, University of Science and Technology of Mazandaran, Behshahr, Iran
⁴⁸ Also at Helwan University, Cairo, Egypt
⁴⁹ Also at Italian National Agency for New Technologies, Energy and Sustainable Economic Development, Bologna, Italy
⁵⁰ Also at Centro Siciliano di Fisica Nucleare e di Struttura Della Materia, Catania, Italy
⁵¹ Also at Università degli Studi Guglielmo Marconi, Roma, Italy
⁵² Also at Scuola Superiore Meridionale, Università di Napoli ‘Federico II’, Napoli, Italy
⁵³ Also at Fermi National Accelerator Laboratory, Batavia, Illinois, U.S.A.
⁵⁴ Also at Università di Napoli ‘Federico II’, Napoli, Italy
⁵⁵ Also at Ain Shams University, Cairo, Egypt
⁵⁶ Also at Consiglio Nazionale delle Ricerche — Istituto Officina dei Materiali, Perugia, Italy
⁵⁷ Also at Riga Technical University, Riga, Latvia
⁵⁸ Also at Department of Applied Physics, Faculty of Science and Technology, Universiti Kebangsaan Malaysia, Bangi, Malaysia
⁵⁹ Also at Consejo Nacional de Ciencia y Tecnología, Mexico City, Mexico
⁶⁰ Also at Trincomalee Campus, Eastern University, Sri Lanka, Nilaveli, Sri Lanka
⁶¹ Also at INFN Sezione di Pavia, Università di Pavia, Pavia, Italy
⁶² Also at National and Kapodistrian University of Athens, Athens, Greece
⁶³ Also at Ecole Polytechnique Fédérale Lausanne, Lausanne, Switzerland
⁶⁴ Also at University of Vienna Faculty of Computer Science, Vienna, Austria
⁶⁵ Also at Universität Zürich, Zurich, Switzerland
⁶⁶ Also at Stefan Meyer Institute for Subatomic Physics, Vienna, Austria
⁶⁷ Also at Laboratoire d’Annecy-le-Vieux de Physique des Particules, IN2P3-CNRS, Annecy-le-Vieux, France
⁶⁸ Also at Near East University, Research Center of Experimental Health Science, Mersin, Turkey
⁶⁹ Also at Konya Technical University, Konya, Turkey
⁷⁰ Also at Izmir Bakircay University, Izmir, Turkey
⁷¹ Also at Adiyaman University, Adiyaman, Turkey
⁷² Also at Necmettin Erbakan University, Konya, Turkey
⁷³ Also at Bozok Universitetesi Rektörlüğü, Yozgat, Turkey
⁷⁴ Also at Marmara University, Istanbul, Turkey
⁷⁵ Also at Milli Savunma University, Istanbul, Turkey
⁷⁶ Also at Kafkas University, Kars, Turkey
⁷⁷ Also at Hacettepe University, Ankara, Turkey
⁷⁸ Also at Istanbul University — Cerrahpasa, Faculty of Engineering, Istanbul, Turkey

- ⁷⁹ Also at Yildiz Technical University, Istanbul, Turkey
⁸⁰ Also at Vrije Universiteit Brussel, Brussel, Belgium
⁸¹ Also at School of Physics and Astronomy, University of Southampton, Southampton, United Kingdom
⁸² Also at University of Bristol, Bristol, United Kingdom
⁸³ Also at IPPP Durham University, Durham, United Kingdom
⁸⁴ Also at Monash University, Faculty of Science, Clayton, Australia
⁸⁵ Now at an institute or an international laboratory covered by a cooperation agreement with CERN
⁸⁶ Also at Università di Torino, Torino, Italy
⁸⁷ Also at Bethel University, St. Paul, Minnesota, U.S.A.
⁸⁸ Also at Karamanoğlu Mehmetbey University, Karaman, Turkey
⁸⁹ Also at California Institute of Technology, Pasadena, California, U.S.A.
⁹⁰ Also at United States Naval Academy, Annapolis, Maryland, U.S.A.
⁹¹ Also at Bingol University, Bingol, Turkey
⁹² Also at Georgian Technical University, Tbilisi, Georgia
⁹³ Also at Sinop University, Sinop, Turkey
⁹⁴ Also at Erciyes University, Kayseri, Turkey
⁹⁵ Also at Horia Hulubei National Institute of Physics and Nuclear Engineering (IFIN-HH), Bucharest, Romania
⁹⁶ Also at Texas A&M University at Qatar, Doha, Qatar
⁹⁷ Also at Kyungpook National University, Daegu, Korea
⁹⁸ Also at another institute or international laboratory covered by a cooperation agreement with CERN
⁹⁹ Also at Universiteit Antwerpen, Antwerpen, Belgium
¹⁰⁰ Also at Yerevan Physics Institute, Yerevan, Armenia
¹⁰¹ Also at Northeastern University, Boston, Massachusetts, U.S.A.
¹⁰² Also at Imperial College, London, United Kingdom
¹⁰³ Also at Institute of Nuclear Physics of the Uzbekistan Academy of Sciences, Tashkent, Uzbekistan